COOPERATIVE GUIDANCE METHOD WITH FORMATION CONTROL FOR A GUIDED MUNITION SWARM

A THESIS SUBMITTED TO
THE GRADUATE SCHOOL OF NATURAL AND APPLIED SCIENCES
OF
MIDDLE EAST TECHNICAL UNIVERSITY

BY

FURKAN ZEKİ AYHAN

IN PARTIAL FULFILLMENT OF THE REQUIREMENTS
FOR
THE DEGREE OF MASTER OF SCIENCE
IN
MECHANICAL ENGINEERING

JANUARY 2023

Approval of the thesis:

COOPERATIVE GUIDANCE METHOD WITH FORMATION CONTROL FOR A GUIDED MUNITION SWARM

submitted by **FURKAN ZEKİ AYHAN** in partial fulfillment of the requirements for the degree of **Master of Science** i**n Mechanical Engineering, Middle East Technical University** by,

Prof. Dr. Halil Kalıpçılar
Dean, Graduate School of **Natural and Applied Sciences** _____

Prof. Dr. M. A. Sahir Arıkan
Head of the Department, **Mechanical Engineering** _____

Assoc. Prof. Dr. Ali Emre Turgut
Supervisor, **Mechanical Engineering Dept., METU** _____

Prof. Dr. Veysel Gazi
Co-Supervisor, **Control and Automation Engineering Dept., Yıldız Technical University** _____

Examining Committee Members:

Assoc. Prof. Dr. A. Buğra Koku
Mechanical Engineering Dept., METU _____

Assoc. Prof. Dr. Ali Emre Turgut
Mechanical Engineering Dept., METU _____

Assoc. Prof. Dr. M. Bülent Özer
Mechanical Engineering Dept., METU _____

Prof. Dr. Veysel Gazi
Control and Automation Engineering Dept., Yıldız Technical University _____

Assoc. Prof. Dr. Can Ulaş Doğruer
Mechanical Engineering Dept., Hacettepe University _____

Date: 27.01.2023

I hereby declare that all information in this document has been obtained and presented in accordance with academic rules and ethical conduct. I also declare that, as required by these rules and conduct, I have fully cited and referenced all material and results that are not original to this work.

Name Last name : Furkan Zeki Ayhan

Signature :

ABSTRACT

COOPERATIVE GUIDANCE METHOD WITH FORMATION CONTROL FOR A GUIDED MUNITION SWARM

Ayhan, Furkan Zeki
Master of Science, Mechanical Engineering
Supervisor: Assoc. Prof. Dr. Ali Emre Turgut
Co-Supervisor: Prof. Dr. Veysel Gazi

January 2023, 91 pages

A cooperative guidance method for a guided munition swarm that contains informed and naïve members is presented in this study. These guided munitions create a swarm with the help of communication between them. The communication of the members is established using RF Datalink, which can transfer a decided set of data between the transmitter and receiver. Since the seeker systems are one of the most expensive parts of a guided munition, using RF Datalink and cooperative guidance methods with formation control for the swarm agents can be a cheaper and more effective way to destroy the desired area. On the other hand, simultaneous attack of multiple smart munitions unavoidably makes it harder to defend an area. 6 degrees of freedom simulation is built to examine the methods and algorithms. The potential function method is applied to achieve formation control and uniform distribution on the horizontal plane. Uniform and safe arm flight is reached due to data transfer between the swarm members. The cooperative guidance method makes the agents follow the same line of sight angle for all naïve agents at the vertical plane. Effects of this guidance method on the heading angle differences, irregularity, and wideness on the horizontal plane through the heading direction are investigated. Results for various

numbers of total agents and various numbers of informed agents are compared. The effects of these on the results are reviewed. The method is proposed as effective for targets positioned in line, such as vehicle convoys.

Keywords: Formation Control, Smart Munition Guidance, Cooperative Guidance Method, Swarm Guidance

ÖZ

GÜDÜMLÜ MÜHİMMAT SÜRÜSÜ İÇİN FORMASYON KONTROLÜ VE BİRLİKTE GÜDÜM YÖNTEMİ

Ayhan, Furkan Zeki
Yüksek Lisans, Makina Mühendisliği
Tez Yöneticisi: Doç. Dr. Ali Emre Turgut
Ortak Tez Yöneticisi: Prof. Dr. Veysel Gazi

Ocak 2023, 91 sayfa

Bu tezde hedef hakkında bilgi sahibi olan ve olmayan elemanlardan oluşan güdümlü mühimmat sürüsü için oluşturulmuş birlikte güdüm yöntemi anlatılmaktadır. Bu güdümlü mühimmatlar birbirleriyle haberleşirken radio frekanslı veri bağı kullanmaktadırlar. Bu veri bağları gönderici ve alıcı arasında belirlenen veri setlerinin akışını sağlayarak mühimmatlar arası iletişimi sağlar. Arayıcı başlık sistemleri güdümlü mühimmatların en pahalı parçalarından biri olması sebebiyle radio frekanslı veri bağları; birlikte güdüm yöntemleri ve formasyon kontrolü ile kullanıldığında bir alanı etkisiz hale getirmek için kullanılabilecek daha ucuz ve etkili bir yöntem olarak değerlendirilebilir. Bunun yanında aynı anda yapılan bu saldırılar korunmak istenen bölgenin hava savunmasını kaçınılmaz olarak zorlaştırmaktadır. 6 serbestlik dereceli simülasyonlar oluşturularak bahsi geçen algoritmalar ve metodlar test edilmiştir. Formasyon kontrolü ile beraber düzenli bir dağılım sağlamak amacıyla potansiyel fonksiyon metodu uygulanmıştır. Sürü üyeleri arasındaki veri paylaşımlarının sonucu olarak düzenli ve güvenli bir kol uçuşu sağlandığı gözlemlenmiştir. Dikey eksende ise birlikte güdüm yöntemi; sürüdeki hedef bilgisi olmayan elemanların, hedef bilgisi olanlar ile aynı görüş hattı açısını

izlemesini sağlamıştır. Bahsi geçen methodun; baş açıları arasındaki farklar, yatay eksendeki pozisyonların düzenliliği ve genişliği üzerindeki etkileri incelenmiştir. Bu parametrelerin değişen toplam sürü üye sayısına ve hedef hakkında bilgisi olan eleman sayısına göre değişimi incelenmiştir. Bu parametrelerin sonuçlar üzerine etkisi değerlendirilmiştir. Yöntem, araç konvoyları gibi sıraya dizilmiş hedefler için etkili olarak önerilmiştir.

Anahtar Kelimeler: Sürü Güdümü, Formasyon Kontrolü, Akıllı Mühimmat Güdümü, Birlikte Güdüm Yöntemleri

To Family and My Love

ACKNOWLEDGMENTS

I want to express my deepest gratitude to my supervisor Assoc. Prof. Dr. Ali Emre Turgut and co-supervisor Prof. Dr. Veysel Gazi, not only for their essential contributions and wise guidance about this study but also for their vast moral support about life. I am grateful for having a chance to meet with them through the concept of the swarm.

I would like to show my respect for the father of Turks, Mustafa Kemal Atatürk, for all the opportunities given by him to our society. Thanks to Roketsan for all the possibilities provided for me to continue my academic education.

I would like to thank my mother, my first teacher, for her endless patience and love, my father for his unlimited support, belief, and leadership, and my brothers for their powerful faith and heartiness toward me. Also, I am so grateful for the support of all the Ayhan and Oğuz family members throughout my life.

My lovely wife Ayşegül, who always stands next to me about everything, deserves the best gratefulness for her beautiful heart. Even when she is fighting an illness, I felt all her support in my soul for years. I will be there for you all the time. I must thank you for being in my life.

TABLE OF CONTENTS

LIST OF TABLES

TABLES

LIST OF FIGURES

FIGURES

LIST OF ABBREVIATIONS

ABBREVIATIONS

CAS: Control Actuator System

DCM: Direction Cosine Matrix

DOF: Degree of Freedom

IMU: Inertial Measurement Unit

INS: Inertial Navigation System

LOS: Line of Sight

PNG: Proportional Navigation Guidance

STT: Skid-to-Turn

PID: Proportional Integral Derivative

IRF: Inertial Reference Frame

BRF: Body Reference Frame

VPG: Velocity Pursuit Guidance

LIST OF SYMBOLS

SYMBOLS

$\hat{C}^{(n,m)}$: DCM matrix from m reference frame to n reference frame

ϕ, θ, ψ: Euler angles for roll, pitch and yaw

p, q, r: Angular velocities for roll, pitch and yaw

α: angle of attack

β: side slip angle

$\vec{r}_{ab}$: Position vector from b to a

X, Y, Z: Aerodynamic forces at body axis

L, M, N: Aerodynamic moments at body axis

u, v, w: Velocity components at body axis

x, y, z: Translational position components at inertial reference frame

k_{nav}: Value of k calculated by navigation algorithms

ω: Angular velocity

λ: Line of sight angle

$\dot{k}$: Time derivative of parameter k

γ: Velocity vector angle wrt inertial reference frame

CHAPTER 1

INTRODUCTION

1.1 Motivation of the Thesis

Group of individuals come together for a purpose and move as one entity, which is called swarm. This behavior is observed in many animals like bees, ants, birds, fish, and bacteria. Living as a group lets the members solve problems that are impossible for them individually [1]. Interaction, communication, and assistance between the group members make it possible to accomplish tasks that are beyond the limit of an individual.

Observation of nature gives us significant information about the behavior of swarms. The purpose of coming together varies for different swarm species. For example, small fish protect themselves easier against a hunter when they create a swarm. Likewise, a group of ants come together and perform huge tasks that are impossible for one of them. They can build huge living and storage areas that any individual in the swarm cannot produce by himself. They store lots of food and stay calm using these nests under the ground. Due to these abilities, the members live under harsh winter circumstances [22,23]. In addition, lions live as a group and attack their victims together and are stronger to increase the chance of catching them. All these various outcomes of living as a swarm make them cooperate and assist each other in nature.

The behavior of various kinds of animals led the way to essential developments in different areas of technology. Munition guidance methods can also use the swarms in nature as a guide. The advantage of being a swarm should be used for munition technology. Using nature as a model, members of the munition swarm guide

themselves and accomplish impossible tasks for a single munition. Guided munitions are also smart technological devices that aim to reach and destroy selected target areas. Application of the knowledge of swarm features on smart munition areas can be very advantageous and helpful. Protecting an area from the simultaneous attack of a guided munition swarm can become very tough. The probability of reaching the target area can be increased with this application on smart munitions.

To apply swarm strategies to a guided munition swarm, Newton's equation of motion for flight dynamics is derived and applied to a munition. 6 degrees of freedom models and simulations are created in MATLAB/SIMULINK program to simulate and analyze the outputs of the system. Different initial conditions are examined, and results are demonstrated with plots. The effect of the total number of agents and informed agent number on the results are investigated for the cooperative guidance method applied.

1.2 Aim of the Thesis

In this thesis, we design a cooperative guidance method for air-to-ground guided munition swarm which is released from UAVs. Air-to-ground munitions are very appropriate for swarm applications when the trajectories of the munitions are regarded. The line-of-sight angle of the munition during flight changes a little, and multiple release opportunities are extensive. UAV platforms are extremely critical and have lots of advantages in the field [27,28]. These platforms can carry multiple munitions together. Therefore, the concept is very applicable for guided munitions.

The usage of data transfer between different platforms is an extremely popular concept these days. This concept is applied to platforms such as unmanned air vehicles, quadrotors, unmanned ground vehicles, and unmanned sea vehicles [25,26]. In addition to this, connections between distinct species are also another vital concept nowadays. Possible advantages of communication between members on the missile guidance concept are considered and active collision avoidance is

desired, and the guidance method proposes uniform, safe and collaborative flight while going toward the target.

In 6 degrees of freedom, the munition swarm is modeled and simulated. Transfer of critical data such as position, acceleration, and velocity of agents are used for these methods. Target is considered a set of objects positioned in line, such as a military convoy or a housing placed nearby.

A cooperative guidance method is applied by providing position control of the swarm agents. Control of the position of an agent is produced using a PID controller and a potential function. In these swarm models, both informed and naïve agents are involved. The results and outputs of the simulations on the MATLAB/SIMULINK application are also demonstrated with figures and tables.

CHAPTER 2

LITERATURE REVIEW

2.1 Swarm Studies

The behavior of swarm agents, properties, and abilities have been investigated by people so far. All these features inspired scientists and engineers for different studies. Distinctive features of the swarm are named, modeled, and analyzed in these studies. For example, self-organization is the emergence of patterns and order in a system by internal processes between members. Çelikkanat and Şahin studied on self-organization of robot flocks for controlling the heading angles [2]. Formation control is the process of positioning the members for the chosen pattern. Murray and Olfati worked on multiple vehicle formation and control [3]. Flocking is the collective motion that occurs to achieve a common purpose while the group members are interacting. Turgut, Huepe, Ferrante, and Gianluca work on the flocking behavior of multi-robot systems using different control methods like elasticity-based mechanism, and null space-based behavior control [4,5]. Aggregation behavior is another basic behavior observed in nature widely between bacteria and insects. Sliding mode control, artificial potential methods, and neighborhood strategies have been studied in the area of swarm aggregation [24].

Swarming behavior in nature also affected the development of technological vehicles. The communication capability of individual vehicles with developing technologies lead humanity to build new concepts. Communication of vehicles created new connections not only for the same type of vehicles but also vehicles that have totally different abilities. Communication between these distinct vehicles is

carried out with various kinds of data transfer systems such as radio frequency data links, wireless fidelity, and Bluetooth.

Communication technology has been used in many different areas. Connection of different technological products has been settled from simple smart home products to military fighters. Members of the system are used to establish a mission that is impossible for only one by itself. One of the most important fields is control technologies for various kinds of vehicles. Cooperative control methods have been used to coordinate the agents of the swarm in harmony. Cooperative control of multivehicle systems is a popular concept for various fields, which include vehicles that can work together for a group purpose. Unmanned ground vehicles, unmanned aerial vehicles, underwater vehicles, autonomous cars, and various kinds of robots are examples of popular vehicles that use these methods.

Different algorithms and control strategies are used to control the formation of quadcopter swarm members [7]. Positioning and guidance strategies are applied to drone systems. UAVs are other flying vehicles that formation control and guidance methods are applied. Multiple UAVs are connected to each other with data transfer, and complex duties are accomplished by these gorgeous systems [6]. Swarm intelligence control mechanisms are used to form a certain path with robots that can move on the ground [8]. A potential field with obstacle avoidance properties is implemented to control and instruct the formation of an unmanned ground vehicle swarm [31]. The swarm that contains autonomous underwater vehicles (AUVs) under the effects of environmental disturbances has been produced so far [9,10]. These applications are part of the examples that technological swarms can succeed. Multiple vehicle applications can make it possible to achieve more challenging missions.

2.2 Missile Guidance Methods

Laser seekers, infrared seekers (IR), and radio frequency (RF) seekers have been used in guided missiles in the past century. Missile guidance concepts have been studied by engineers. As a result, many types of initial, midcourse, and terminal guidance methods have been produced for missiles with these different seeker concepts. One of the most popular guidance methods is proportional navigation guidance (PNG). This guidance method uses line-of-sight angle rate to create commands while moving through the target. The method creates acceleration commands so that the line-of-sight angle rate converges to 0. Another popular guidance method is velocity pursuit guidance. This method creates acceleration commands to change the unit vector of the missile's velocity to overlap with the unit vector of the missile to the target vector [32]. Both methods are successfully applied for particular purposes of guided munitions, rockets, spacecrafts, and missiles.

Missile guidance techniques not only made it available to hit the target but also made multiple features available. Control of impact angle and time might be desirable for military purposes. Missile guidance and control strategies have been used to control impact angle and impact time [11,12,13,14]. The guidance law named Impact Time Control Guidance has been offered with different application methods. For an air defense system opposing multiple threats at the same time is not easy in many aspects. Tracking all the airfield threats and making interception available for them requires advanced technologies. Simultaneous attack of multiple missiles is aimed by adding impact time error feedback to the proportional navigation guidance command [15] and using a bias term including impact time error added to proportional navigation guidance [16]. To satisfy the simultaneous arrival, Lyapunov-based guidance law for impact time control is also used [17].

As missile guidance methods and technologies have been upgraded in time, anti-missile systems have been developed too. GPS jammers, hit-to-kill air defense missiles, and decoy flares are examples of the precautions used for missile defense. The range of radars of the air defense systems increased in time with growing

technology. Also, defense missile technology has been developed, and the range of the missiles has increased in time. Active and semi-active radar seeker systems used in the missiles improved and supplied less noisy and precise target-related data to the system. In addition, proximity sensors have evolved to sense the target within a range and cleared off the necessity of precisely hitting the target to beat it. Furthermore, the effective range of warheads has increased in time with the knowledge accumulated in time.

Triangle intercept guidance, proportional navigation guidance, the command to line of sight guidance, and its derivatives have been used as guidance methods for aerial attacks [33]. To reach the target, a multi-munition attack can be preferred. Using more than one munition to attack increases the chance of breaking through the possible anti-missile systems. And some of the munitions can be used without the seeker, which is one of the most expensive parts of the munition. Munition swarms contain a munition with complete equipment and seeker-less munitions are cost-effective in this concept. Attacking with more than one munition together means more than one enemy to overcome for the defense system. As a result of this opinion, munition swarms can be preferred for essential targets.

In recent times when military drones are trending vehicles, the munition swarms are very convenient for multiple attack. The possibility of carrying multiple munitions together with one military drone and communication properties for military drone systems make it extremely easy to implement a swarm for munitions. The absence of a propeller system for a munition comes with numerous advantages in the field of price and convenience of controllability.

2.3 Contribution of the Thesis

In this thesis, a cooperative guidance method for air-to-ground munition swarm is proposed. In this method, uniformity on the horizontal plane towards the target and convergence on the line-of-sight angles at a certain angle on the vertical plane is desired. The cooperative guidance method and position control algorithms with a potential function method are applied for the first time in the literature.

All these methods are implemented to a 6-degree of freedom model for each agent of the swarm. Number of total agents and informed agents on the swarm are also changed to simulate different conditions. The effects of changing numbers of total and informed agents are analyzed.

Metrics that advise about uniformity, wideness, and heading angle variation of the swarm are created. The effect of the guidance method on these metrics is studied for the first time. Several different conditions are simulated using the MATLAB/Simulink application and results are plotted in the following sections.

CHAPTER 3

MODELLING AND SIMULATION

3.1 Reference Frames in 6-DOF

Mathematical operations and calculations are performed using vectors in 6 degrees of freedom equations related to the motion of a single munition. These vectors are meaningful when they are defined at predefined reference frames. In these simulations, different reference frames are needed to implement the methods.

3.1.1 Body Fixed Reference Frame

The body fixed reference frame is a reference frame that is attached to the center of gravity of the body and moves with the body. It is a right-handed frame in which the x-axis shows the nose of a body, and the z-axis shows the downside while making 90° with the x-axis. And since it is a right-handed reference frame, the y-axis points the direction where the x axis is rotated around the z axis 90° in the positive direction.

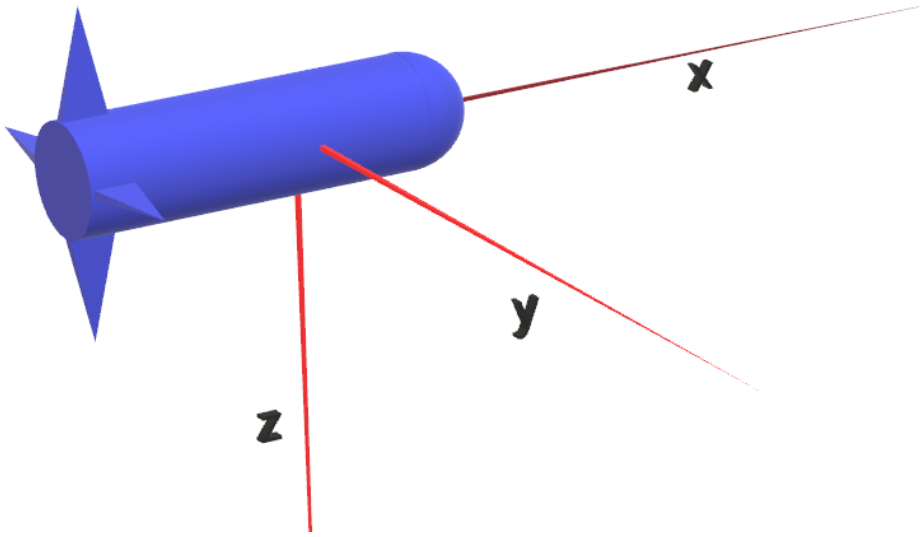

Figure 1 Body fixed frame

3.1.2 Inertial Reference Frame

The inertial reference frame is a fixed and non-moving reference frame that the x-direction shows the initial nose direction of the body, the z-direction shows the ground, and the y-direction is placed according to the right-hand rule. This reference frame is placed on the ground at the point where the body starts the motion. Therefore, the body might start its motion at different altitudes according to the inertial reference frame, but it starts from 0 at x and y-directions. IRF is placed according to the munition at the center for swarm applications. Therefore, the munition at the center starts its motion from 0 x and y positions with known altitude. All the notations that will be operated are consistent with the notation presented by Özgören [18].

3.2 Vectors and Transformation matrices in 6-DOF

The munition starts its motion from an initial position, and the body reference frame moves in time at the center of gravity with the munition. The motion of the body with respect to IRF can be shown as follows:

Inertial position vector at inertial reference frame:

$$\bar{r}^{(i)} = \{\vec{r}_{b/i}\}^{(i)} = \begin{bmatrix} x_i \\ y_i \\ z_i \end{bmatrix} \tag{1}$$

Initial positions at inertial reference frame:

$$\bar{r}_0{}^{(i)} = \{\vec{r}_{b/i}(0)\}^{(i)} = \begin{bmatrix} x_i(0) \\ y_i(0) \\ z_i(0) \end{bmatrix} \tag{2}$$

Euler angles are defined between the inertial reference frame and the body reference frame. The rotation angle around the x-axis is called ϕ, the rotation angle around the y-axis is called θ, and the rotation angle around the z-axis is called ψ angle. Euler angles are considered as starting from 0 angle at each axis in general.

Initial Euler angles can be written as:

$$\Gamma_0 = \begin{bmatrix} \phi_0 \\ \theta_0 \\ \psi_0 \end{bmatrix} \tag{3}$$

The translational velocity vector on the body fixed frame is:

$$\bar{V}^{(b)} = \left\{\vec{V}_{b/i}\right\}^{(b)} = \begin{bmatrix} u \\ v \\ w \end{bmatrix} \tag{4}$$

The angular velocity vector on the body fixed frame is:

$$\bar{\omega}^{(b)} = \left\{\vec{\omega}_{b/i}\right\}^{(b)} = \begin{bmatrix} p \\ q \\ r \end{bmatrix} \tag{5}$$

Different reference frames are used in this study; therefore, transformation matrices are created to transform vectors while making different calculations about navigation, guidance, and control. Rotation matrices at distinct axes can be written separately.

Rotation matrice around the x-axis can be written as:

$$\hat{R}_1(\phi) = e^{\tilde{u}_1 \phi} = \begin{bmatrix} 1 & 0 & 0 \\ 0 & \cos(\phi) & -\sin(\phi) \\ 0 & \sin(\phi) & \cos(\phi) \end{bmatrix} \tag{6}$$

Rotation matrice around the y-axis can be written as:

$$\hat{R}_2(\theta) = e^{\tilde{u}_2 \theta} = \begin{bmatrix} \cos(\theta) & 0 & \sin(\theta) \\ 0 & 1 & 0 \\ -\sin(\theta) & 0 & \cos(\theta) \end{bmatrix} \tag{7}$$

Rotation matrice around the z-axis can be written as:

$$\hat{R}_3(\psi) = e^{\tilde{u}_3 \psi} = \begin{bmatrix} \cos(\psi) & -\sin(\psi) & 0 \\ \sin(\psi) & \cos(\psi) & 0 \\ 0 & 0 & 1 \end{bmatrix} \tag{8}$$

In 6-DOF, the transformation matrix between the body fixed and inertial frame can be expressed by multiplying all the single rotation matrices shown before.

$$\hat{C}^{(i,b)} = \hat{R}_3(\psi)\hat{R}_2(\theta)\hat{R}_1(\phi) \tag{9}$$

$$\hat{C}^{(i,b)} = \begin{bmatrix} (\mathrm{c}\psi\mathrm{c}\theta) & (\mathrm{c}\psi\, s\theta\, \mathrm{s}\phi - \mathrm{s}\psi\, \mathrm{c}\phi) & (\mathrm{c}\,\psi\, \mathrm{s}\theta\, \mathrm{c}\phi + \mathrm{s}\psi\, \mathrm{s}\phi) \\ (s\psi\, \mathrm{c}\theta) & (\mathrm{s}\psi\, \mathrm{s}\theta\, \mathrm{s}\phi + \mathrm{c}\psi\, \mathrm{c}\phi) & (\mathrm{s}\,\psi\, \mathrm{s}\theta\, \mathrm{c}\phi - \mathrm{c}\psi\, \mathrm{s}\phi) \\ -\mathrm{s}\theta & (\mathrm{c}\theta\, \mathrm{s}\phi) & (\mathrm{c}\theta\, \mathrm{c}\phi) \end{bmatrix} \tag{10}$$

$$\hat{C}^{(b,i)} = \left[\hat{C}^{(i,b)}\right]^T \tag{11}$$

Translational Velocity Derivative Vector on BRF:

$$\dot{\vec{V}}^{(b)} = \frac{d}{dt}\vec{V}_{b/i}\Big|_b^{(b)} = \begin{bmatrix} \dot{u} \\ \dot{v} \\ \dot{w} \end{bmatrix} \tag{12}$$

Translational Velocity Derivative Vector on BRF:

$$\bar{a}^{(b)} = \frac{d}{dt}\vec{V}_{b/i}\Big|_I^{(b)} = \begin{bmatrix} a_x \\ a_y \\ a_z \end{bmatrix} \tag{13}$$

Rotational Velocity Derivative Vector on BRF:

$$\dot{\bar{\omega}}^{(b)} = \frac{d}{dt}\vec{\omega}_{b/i}\Big|_b^{(b)} = \begin{bmatrix} \dot{p} \\ \dot{q} \\ \dot{r} \end{bmatrix} \tag{14}$$

Using DCM matrices, Euler angles can be subtracted.

Euler angle calculation around the roll axis:

$$\phi = \mathrm{atan}\left(\frac{\hat{C}^{(b,i)}(2,3)}{\hat{C}^{(b,i)}(3,3)}\right) \tag{15}$$

where ϕ is defined at $[-\pi, \pi]$,

Euler angle calculation on the pitch axis is calculated as:

$$\theta = \text{atan}\left(\frac{-\hat{C}^{(b,i)}(1,3)}{\sqrt{\hat{C}^{(b,i)}(3,3)^2 + \hat{C}^{(b,i)}(2,3)^2}}\right) \tag{16}$$

where θ is defined at $[-\frac{\pi}{2}, \frac{\pi}{2}]$,

Euler angle calculation on the yaw axis is calculated as:

$$\psi = \text{atan}\left(\frac{\hat{C}^{(b,i)}(1,2)}{\hat{C}^{(b,i)}(1,1)}\right) \tag{17}$$

where ψ is defined at $[-\pi, \pi]$.

3.3 Parameter Calculations Related with Aerodynamics

Angle of attack, sideslip angle, and mach number have a direct effect on aerodynamic force and moments. Therefore, these parameters have to be calculated to model the motion of the body.

The speed of sound is calculated using the atmosphere model. It is shown with a for calculations. Mach number is calculated using the magnitude of translational velocity and speed of sound.

$$M = \frac{|\vec{V}_{b/i}|}{a} \tag{18}$$

Airplanes, helicopters, drones, missiles, or munitions do not always move toward where their body of them shows. In general, because of the body's motion, air particles come with a relative velocity V_{inf} with respect to the body. Angles between the wind and the body of the munition are defined at two axes separately. The angle at the pitch axis is called the angle of attack and it is shown with α. Angle at the yaw axis is called the side slip angle and it is shown with β.

The angle of attack on the body is shown in Figure 2.

Figure 2 Angle of attack

The angle of attack is calculated as follows:

$$\alpha = \text{atan}\left(\frac{w}{u}\right) \tag{19}$$

The sideslip angle on the body is shown in Figure 3:

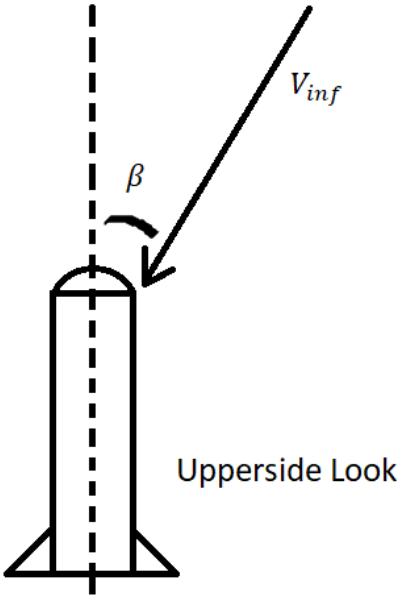

Figure 3 Sideslip Angle

The sideslip angle is calculated as follows:

$$\beta = \text{asin}\left(\frac{v}{|\vec{V}_{b/i}|}\right) \tag{20}$$

3.4 Physical Properties of Munition

The physical properties of the munition are taken as shown in Table 1.

Table 1 Physical properties

m=25 kg
$I_{xx} = 0.08\ kgm^2$
$I_{yy} = 0.98\ kgm^2$
$I_{yy} = 0.98\ kgm^2$
$I_{xy} = I_{xz} = I_{yz} = 0$
$S_{ref} = 0.0177m^2$
$l_{ref} = 0.15$m

3.5 Aerodynamic Forces and Moments

Aerodynamic forces and moments are defined at the body fixed frame.

Aerodynamic forces are shown as:

$$\vec{F}_{aero} = \begin{bmatrix} X \\ Y \\ Z \end{bmatrix} \tag{21}$$

Aerodynamic moments are shown as:

$$\vec{M}_{aero} = \begin{bmatrix} L \\ M \\ N \end{bmatrix} \tag{22}$$

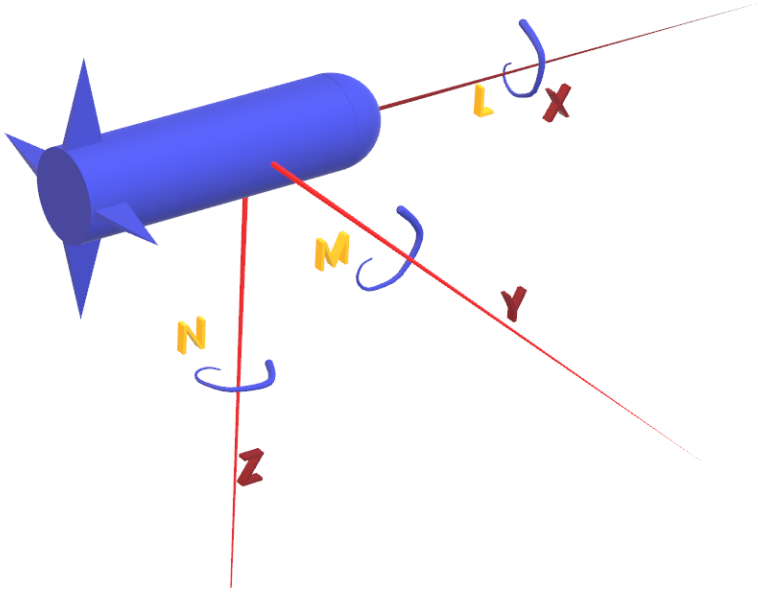

Figure 4 Aerodynamic forces and moments

All these aerodynamic forces and moments change according to Mach number, angle of attack, sideslip angle, and deflection angles of control surfaces at the back side of the body. In this study, DATCOM program outputs for a single munition are created. DATCOM is a computer program used to calculate aerodynamic properties, static stability, and control characteristics of any design. The program takes the geometry of a design and creates the aerodynamic data accordingly. The aerodynamic data outputs are linearized, and aerodynamic forces and moments are calculated. Aerodynamic derivatives are considered the same for all Mach numbers.

Table 2 Aerodynamic coefficient derivatives

$C_{Y_\delta} = -14.32$	$C_{Y_\beta} = -22.91$
$C_{Z_\delta} = -14.32$	$C_{Z_\alpha} = -22.91$
$C_{L_\delta} = -1.72$	$C_{L_p} = -14$
$C_{M_\delta} = -28.65$	$C_{M_\alpha} = -11.46$
$C_{N_\delta} = 28.65$	$C_{N_\beta} = 11.46$
$C_{X_0} = -1.2$	$C_{Z_q} = C_{Y_r} = 0$

Aerodynamic coefficients $C_Z, C_Y, C_X, C_L, C_M, C_N$ are taken as linearly changing with related control surface, related angular velocity and related angle of attack on the channel. Related control surface on the pitch axis is named as elevator deflection shown with δ_e. Related control surface on the yaw axis is named as rudder deflection shown with δ_r. Related control surface on the roll axis is named as aileron deflection shown with δ_a. It can be shown with the following equations.

$$C_X = C_{X_0} \tag{23}$$

$$C_Y = C_{Y_\delta}\delta_r + C_{Y_\beta}\beta \tag{24}$$

$$C_Z = C_{Z_\delta}\delta_e + C_{Z_\alpha}\alpha \tag{25}$$

$$C_L = C_{L_\delta}\delta_a + C_{L_p}p \tag{26}$$

$$C_M = C_{M_\delta}\delta_e + C_{M_\alpha}\alpha \tag{27}$$

$$C_N = C_{N_\delta}\delta_r + C_{N_\beta}\beta \tag{28}$$

Dynamic pressure for a munition is calculated as follows.

$$Q = \frac{1}{2}\rho V^2 \tag{29}$$

Derivatives of forces are calculated by multiplying the coefficients with reference area and dynamic pressure. For static moments, derivatives of moments are calculated by multiplying the coefficients with reference area, dynamic pressure, and reference length. For dynamic moments, it is calculated by multiplying with length times, 0.5 times velocity additional to the static moments. One example for each is given in the following equations.

$$Z_\alpha = QS_{ref}C_{Z_\alpha} \tag{30}$$

$$M_\alpha = QS_{ref}l_{ref}C_{Z_\alpha} \tag{31}$$

$$M_q = \frac{QS_{ref}l_{ref}^2 V}{2}C_{Z_\alpha} \tag{32}$$

Aerodynamic forces:

$$X = X_0 \tag{33}$$

$$Y = Y_\beta \beta + Y_\delta \delta_r + Y_r r \tag{34}$$

$$Z = Z_{\alpha} \alpha + Z_\delta \delta_e + Z_q q \tag{35}$$

Aerodynamic moments:

$$L = L_{p} p + L_\delta \delta_a \tag{36}$$

$$M = M_{\alpha} \alpha + M_\delta \delta_e + M_q q \tag{37}$$

$$N = N_\beta \beta + N_\delta \delta_r + N_r r \tag{38}$$

Newton's 6-DOF equation of motion can be written as [19]:

$$\sum \vec{F}_{b/i}^{(b)} = m\vec{a}_{b/i}^{(b)} = m\left(\dot{\vec{V}}_{b/i}^{(b)} + \vec{\omega}_{b/i}{}^{(b)} \times \vec{V}_{b/i}^{(b)}\right) \tag{39}$$

$$X - mg\sin\theta = m[\dot{u} + qw - rv] \tag{40}$$

$$Y + mg\ cos\theta\ sin\phi = m[\dot{v} + ru - pw] \tag{41}$$

$$Z + g\ cos\theta\ cos\phi = m[\dot{w} + pv - qu] \tag{42}$$

$$\sum \vec{M}^{(b)} = \left(\dot{\vec{H}}^{(b)} + \vec{\omega}^{(b)} \times \vec{H}^{(b)}\right) \tag{43}$$

$$L = I_x\dot{p} - I_{yz}(q^2 - r^2) - I_{zx}(\dot{r} + pq) - I_{xy}(\dot{q} - rp) - \left(I_y - I_z\right)qr \tag{44}$$

$$M = I_y\dot{q} - I_{zx}(r^2 - p^2) - I_{xy}(\dot{p} + qr) - I_{yz}(\dot{r} - pq) - (I_z - I_x)rp \tag{45}$$

$$N = I_z\dot{r} - I_{xy}(p^2 - q^2) - I_{yz}(\dot{q} + rp) - I_{zx}(\dot{p} - qr) - \left(I_x - I_y\right)pq \tag{46}$$

AUTOPILOT AND NAVIGATION

4.1 Autopilot Design

Autopilot design starts with producing open-loop matrices. These matrices depend on the aerodynamic data and physical properties of the body. The motion of the body is separated into different channels. Yaw, pitch, and rolling motion are handled and designed for each separately.

4.1.1 Control Surface Actuators

Control surface actuators have their own dynamics to realize given angle command. Motion of the actuator can be modeled using 2nd degree transfer function as shown:

$$\frac{\delta}{\delta_{com}} = \frac{\omega_{act}^2}{s^2 + 2\zeta_{act}\omega_{act}s + \omega_{act}^2} \tag{47}$$

ω_{act} is taken as 18 Hz and ζ_{act} is taken as 0.92. For all control surface angles ($\delta_e, \delta_r, \delta_a$) the same model is used.

4.1.2 Open-Loop Matrices

Dividing the motion of the body into three parts and linearizing the equations, we get the open-loop matrices. Pitching matrices may be created when the states are taken as $w, q, \delta_e, \dot{\delta}_e$. These matrices are derived from Newton's 2nd law of motion written before. The munition autopilot system is designed according to skid-to-turn control method. STT maneuvers are made without a rolling rate on body. Therefore, the rolling rate is taken as 0 while creating open-loop matrices.

$$\begin{bmatrix} \dot{w} \\ \dot{q} \\ \dot{\delta}_e \\ \ddot{\delta}_e \end{bmatrix} = \begin{bmatrix} \frac{Z_\alpha}{mu} & u & \frac{Z_\delta}{m} & 0 \\ \frac{M_\alpha}{I_{yy}u} & \frac{M_q}{I_{yy}} & \frac{M_\delta}{I_{yy}} & 0 \\ 0 & 0 & 0 & 1 \\ 0 & 0 & -\omega_n^2 & -2\zeta\omega_n \end{bmatrix} \begin{bmatrix} w \\ q \\ \delta_e \\ \dot{\delta}_e \end{bmatrix} + \begin{bmatrix} 0 \\ 0 \\ 0 \\ \omega_n^2 \end{bmatrix} \delta_e \tag{48}$$

The open-loop pitch matrix states are changed from x′ to x̂ using the transformation matrix T as shown in equations (49-54) [20]. The munition has an acceleration autopilot at the pitch channel; therefore, the usage of acceleration as a state makes it simpler for autopilot design.

$$x' = \begin{bmatrix} w \\ q \\ \delta_e \\ \dot{\delta}_e \end{bmatrix}, \hat{x} = \begin{bmatrix} a_z \\ q \\ \delta_e \\ \dot{\delta}_e \end{bmatrix}$$

$$\dot{x}' = A'x' + B_u \tag{49}$$

$$\hat{x} = Tx' = \begin{bmatrix} \frac{Z_\alpha}{um} & 0 & \frac{Z_\delta}{m} & 0 \\ 0 & 1 & 0 & 0 \\ 0 & 0 & 1 & 0 \\ 0 & 0 & 0 & 1 \end{bmatrix} \begin{bmatrix} w \\ q \\ \delta_e \\ \dot{\delta}_e \end{bmatrix} = \begin{bmatrix} a_z \\ q \\ \delta_e \\ \dot{\delta}_e \end{bmatrix} \tag{50}$$

$$\dot{x'} = A'x' + B_u u \tag{51}$$

$$x' = T^{-1}\hat{x} \tag{52}$$

$$\dot{\hat{x}} = T\dot{x'} = T(A'x' + B_u u) = TA'T^{-1}\hat{x} + T\hat{B}_u u \tag{53}$$

$$\hat{A} = TA'T^{-1} \tag{54}$$

Yawing motion open-loop matrices are created as the same with the pitching motion. At first, open-loop yaw matrices are created with the states are taken as $v, r, \delta_r, \dot{\delta}_r$.

$$\begin{bmatrix} \dot{v} \\ \dot{r} \\ \dot{\delta}_r \\ \ddot{\delta}_r \end{bmatrix} = \begin{bmatrix} \frac{Y_\beta}{mu} & -u & \frac{Y_\delta}{m} & 0 \\ \frac{N_\beta}{I_{zz}u} & \frac{N_r}{I_{zz}} & \frac{N_\delta}{I_{zz}} & 0 \\ 0 & 0 & 0 & 1 \\ 0 & 0 & -\omega_n^2 & -2\zeta\omega_n \end{bmatrix} \begin{bmatrix} v \\ r \\ \delta_r \\ \dot{\delta}_r \end{bmatrix} + \begin{bmatrix} 0 \\ 0 \\ 0 \\ \omega_n^2 \end{bmatrix} \delta_r \tag{55}$$

States of the open-loop yaw matrix are changed from x′ to x̂ using the transformation matrix T as shown in equations (56-61) [20]. The munition will have an acceleration autopilot at the yaw channel; therefore, using yaw acceleration as a state makes it simpler for autopilot design.

$$x' = \begin{bmatrix} v \\ r \\ \delta_r \\ \dot{\delta}_r \end{bmatrix}, \hat{x} = \begin{bmatrix} a_y \\ r \\ \delta_r \\ \dot{\delta}_r \end{bmatrix}$$

$$\dot{x}' = A'x' + B_u \tag{56}$$

$$\hat{x} = Tx' = \begin{bmatrix} \frac{Y_\beta}{um} & 0 & \frac{Y_\delta}{m} & 0 \\ 0 & 1 & 0 & 0 \\ 0 & 0 & 1 & 0 \\ 0 & 0 & 0 & 1 \end{bmatrix} \begin{bmatrix} v \\ r \\ \delta_r \\ \dot{\delta}_r \end{bmatrix} = \begin{bmatrix} a_y \\ r \\ \delta_r \\ \dot{\delta}_r \end{bmatrix} \tag{57}$$

$$\dot{x'} = A'x' + B_u u \tag{58}$$

$$x' = T^{-1}\hat{x} \tag{59}$$

$$\dot{\hat{x}} = T\dot{x'} = T(A'x' + B_u u) = TA'T^{-1}\hat{x} + T\hat{B}_u u \tag{60}$$

$$\hat{A} = TA'T^{-1} \tag{61}$$

Rolling motion matrices are simpler when it is compared with pitch and yaw channel. States of roll are taken as $\int p, p, \delta_a, \dot{\delta}_a$. Roll dynamics consist of actuator dynamics and rolling rate dynamics. First state is just an integral of rolling rate.

Rolling matrices can be written as:

$$\frac{d}{dt}\begin{bmatrix}\phi\\ p\\ \delta_a\\ \dot{\delta}_a\end{bmatrix}=\begin{bmatrix}0 & 1 & 0 & 0\\ 0 & \frac{L_p}{I_{xx}} & \frac{L_\delta}{I_{xx}} & 0\\ 0 & 0 & 0 & 1\\ 0 & 0 & -\omega_n^2 & -2\zeta\omega_n\end{bmatrix}\begin{bmatrix}\phi\\ p\\ \delta_a\\ \dot{\delta}_a\end{bmatrix}+\begin{bmatrix}0\\ 0\\ 0\\ \omega_n^2\end{bmatrix}\delta_a \qquad (62)$$

4.1.3 Design of Autopilots

4.1.3.1 Roll Channel Design

The open-loop matrix at the roll channel has four states: integral of rolling rate, rolling rate, deflection angle, and derivative of deflection angle. Rolling channel autopilot is designed as an angle tracker. Therefore, the design of the tracker is made using a state feedback controller with an extra state which is integral to the angle error. The state space representation of the design matrix is written as [20]:

$$\frac{d}{dt}\begin{bmatrix}\phi\\ p\\ \delta_a\\ \dot{\delta}_a\\ \int(\phi_{com}-\phi)\end{bmatrix}=\begin{bmatrix}A_{ol}(1,1) & A_{ol}(1,2) & A_{ol}(1,3) & A_{ol}(1,4) & 0\\ A_{ol}(2,1) & A_{ol}(2,2) & A_{ol}(2,3) & A_{ol}(2,4) & 0\\ A_{ol}(3,1) & A_{ol}(3,2) & A_{ol}(3,3) & A_{ol}(3,4) & 0\\ A_{ol}(4,1) & A_{ol}(4,2) & A_{ol}(4,3) & A_{ol}(4,4) & 0\\ -1 & 0 & 0 & 0 & 0\end{bmatrix}\begin{bmatrix}\phi\\ p\\ \delta_a\\ \dot{\delta}_a\\ \int(\phi_{com}-\phi)\end{bmatrix}+\begin{bmatrix}0 & 0\\ 0 & 0\\ 0 & 0\\ \omega_n^2 & 0\\ 0 & 1\end{bmatrix}*\begin{bmatrix}\delta_a\\ \phi_{com}\end{bmatrix}^T \qquad (63)$$

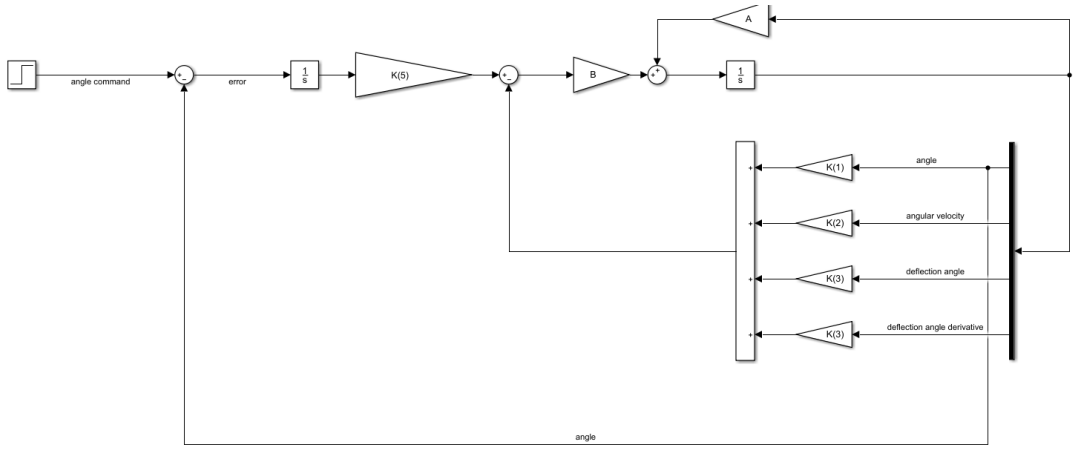

Figure 5 Roll autopilot scheme

Poles of closed-loop are placed according to open-loop pole locations. Open-loop pole locations related with the actuator remain the same. The natural frequency of open-loop pole location associated with the rolling rate is used as a guide frequency. One of the poles other than the actuator poles is placed at the real axis with five times increased natural frequency; the other two poles are placed at five times increased natural frequency and 0.92 damping constant. As a result, there are three poles at the same natural frequency placed radially and two poles placed at their initial location. Gains are calculated using the ‘acker’ code of the MATLAB program.

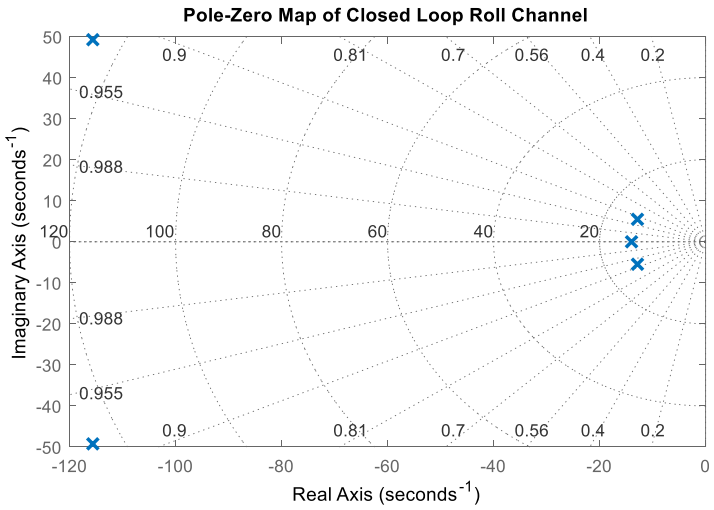

Figure 6 Closed-loop pole-zero map for roll autopilot

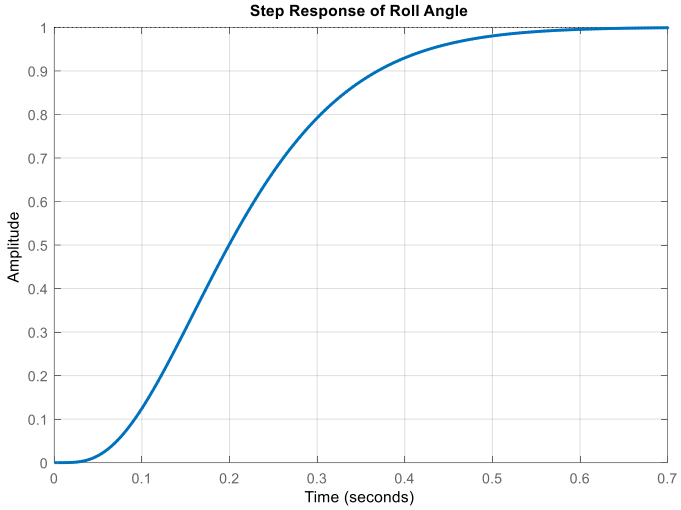

Figure 7 Roll autopilot step response

Step response does not have any overshoot or undershoot according to this design. A damped autopilot design is preferred.

4.1.3.2 Pitch and Yaw Channel Design

The open-loop matrix at the pitch and yaw channel has four states: acceleration, angular rate, deflection angle, and derivative of deflection angle. The autopilot is designed as an acceleration command tracker. Therefore, the design of the tracker is made using a state feedback controller with an extra state which is integral to the acceleration error. The state space representation of the design matrix for the pitch channel is written as [20]:

$$\frac{d}{dt}\begin{bmatrix} \mathrm{a} \\ q \\ \delta_e \\ \dot{\delta}_e \\ \int(a_{com}-a) \end{bmatrix} = \begin{bmatrix} A_{ol}(1,1) & A_{ol}(1,2) & A_{ol}(1,3) & A_{ol}(1,4) & 0 \\ A_{ol}(2,1) & A_{ol}(2,2) & A_{ol}(2,3) & A_{ol}(2,4) & 0 \\ A_{ol}(3,1) & A_{ol}(3,2) & A_{ol}(3,3) & A_{ol}(3,4) & 0 \\ A_{ol}(4,1) & A_{ol}(4,2) & A_{ol}(4,3) & A_{ol}(4,4) & 0 \\ -1 & 0 & 0 & 0 & 0 \end{bmatrix} \begin{bmatrix} \mathrm{a} \\ q \\ \delta_e \\ \dot{\delta}_e \\ \int(a_{com}-a) \end{bmatrix} + \begin{bmatrix} 0 & 0 \\ 0 & 0 \\ 0 & 0 \\ \omega_n^2 & 0 \\ 0 & 1 \end{bmatrix} * \begin{bmatrix} \delta_e \\ a_{com} \end{bmatrix}^T \quad (64)$$

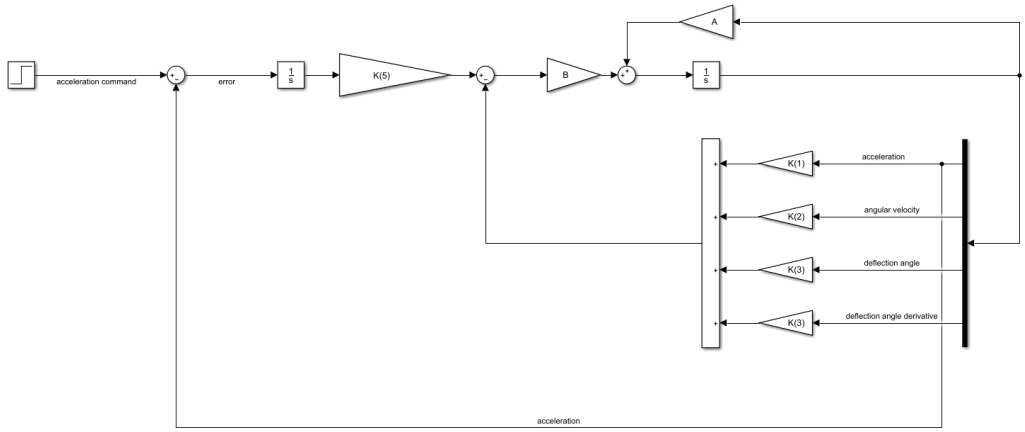

Figure 8 Acceleration autopilot scheme

Poles of the closed-loop are placed according to open-loop pole locations. Open-loop pole locations related with the actuator remain the same for acceleration trackers too. The natural frequency of open-loop pole locations that are closer to the imaginary axis is used as a guide frequency. One of the poles other than the actuator poles is placed at the real axis with the same natural frequency, other two poles are placed at the same natural frequency with a 0.9 damping constant. As a result, there are three poles at the same natural frequency placed radially and two poles placed at their initial location. Gains are calculated using the 'acker' code of the MATLAB program again.

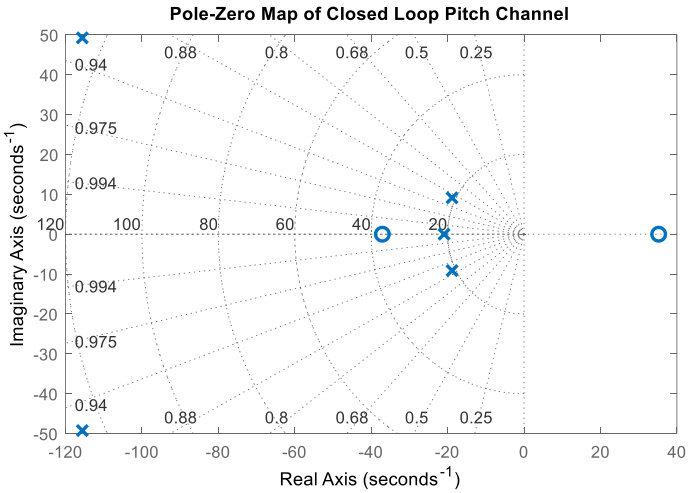

Figure 9 Closed-loop pole-zero map for acceleration autopilots

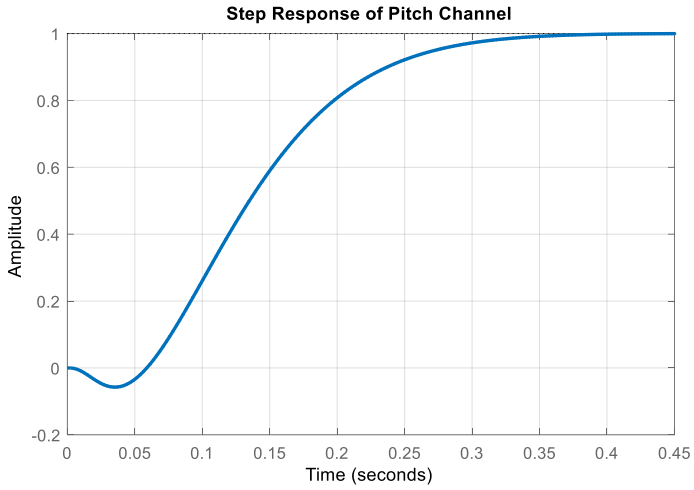

Figure 10 Acceleration autopilot step response

Since the body is thought symmetric at the y-z plane, yaw and pitch channels have the same open-loop characteristic. Therefore, the design of the yaw channel is done the same with the pitch channel for simplicity. There is no overshoot for the step response and a little undershoot. Undershoot comes because of the open-loop dynamics of acceleration.

4.2 Navigation

Application of autopilots and guidance methods require navigation outputs. Sensors at the munition, such as gyro and accelerometer, are used to measure the motion of the body. Accelerometer measurement is modeled as it has a Gaussian distributed noise on the real accelerations that the body has according to the equations of motion in 6D. Similarly, gyro measurement is modeled as it has a Gaussian distributed noise on the real angular velocities that the body has according to the equations of motion in 6D. The rotation of the earth is not included in the calculations related to navigation because of its negligible effect on the results.

4.2.1 Euler Angle Calculation

Subscript k's belong to the kth step of navigation. Initial Euler angles and transformation matrices can be written as:

$$\Gamma_{0_{nav}} = \begin{bmatrix} \phi_0 \\ \theta_0 \\ \psi_0 \end{bmatrix}, \Gamma_{k_{nav}} = \begin{bmatrix} \phi_k \\ \theta_k \\ \psi_k \end{bmatrix} \tag{65}$$

$$\hat{C}_0^{(i,b)}{}_{nav} = \hat{R}_3(\psi_0)\hat{R}_2(\theta_0)\hat{R}_1(\phi_0) \tag{66}$$

$$L_{k_{nav}} = \begin{bmatrix} 1 & \sin(\phi_k)\tan(\theta_k) & \cos(\phi_k)\tan(\theta_k) \\ 0 & \cos(\phi_k) & -\sin(\phi_k) \\ 0 & \sin(\phi_k)\sec(\theta_k) & \cos(\phi_k)\sec(\theta_k) \end{bmatrix} \tag{67}$$

Measured angular velocities are used to calculate Euler angles. Integration of Euler angles is made as [19]:

$$\dot{\Gamma}_{k_{nav}} = \begin{bmatrix} \dot{\phi}_k \\ \dot{\theta}_k \\ \dot{\psi}_k \end{bmatrix} = L_{k_{nav}}\omega_{gyro} \tag{68}$$

$$\Gamma_{k+1_{nav}} = \dot{\Gamma}_{k_{nav}}dt + \Gamma_{k_{nav}} \tag{69}$$

$$\hat{C}_k^{(i,b)}{}_{nav} = \hat{R}_3\left(\psi_{k_{nav}}\right)\hat{R}_2\left(\theta_{k_{nav}}\right)\hat{R}_1\left(\phi_{k_{nav}}\right) \tag{70}$$

$$\hat{C}_k^{(b,i)}{}_{nav} = \left(\hat{C}_k^{(i,b)}{}_{nav}\right)^T \tag{71}$$

4.2.2 Inertial Position Calculation

Inertial position calculation is made using transformation matrices which are calculated with previously calculated Euler angles. Transforming measured acceleration on the body to the inertial reference frame and adding gravity, acceleration on the inertial frame is reached. Integrating acceleration on the inertial reference frame, velocity on the inertial reference frame is calculated. Velocity on an inertial reference frame starts with an initial velocity that has only x component. That component belongs to the forward direction. The inertial position is calculated by integrating velocity on an inertial reference frame [19].

$$V_{0_{nav}}^{\ i} = \begin{bmatrix} V_{x_0} \\ 0 \\ 0 \end{bmatrix}, V_{k_{nav}}^{\ i} = \begin{bmatrix} V_{x_k} \\ V_{y_k} \\ V_{z_k} \end{bmatrix} \tag{72}$$

$$\hat{C}_k^{(i,b)}{}_{nav} a_{acc} + g^i = a_{k_{nav}}^i \tag{73}$$

$$V_{k+1_{nav}}^i = a_{k_{nav}}^i dt + V_{k_{nav}}^i \tag{74}$$

$$V_{k+1_{nav}}^b = \hat{C}_k^{(b,i)}{}_{nav} V_{k+1_{nav}}^i \tag{75}$$

$$p_{k+1_{nav}}^i = V_{k_{nav}}^i dt + p_{k_{nav}}^i \tag{76}$$

CHAPTER 4

COOPERATIVE GUIDANCE METHOD

In this munition swarm concept, some of the munitions are considered as they know the position of the target precisely. These munitions are named ‘informed agents’ in this study. These agents are considered a fully equipped and more expensive type of munition with a seeker system on them. The rest of the agents are considered as they do not have any seeker system, but they can interact with other agents with an RF data link on them. These agents are named ‘naïve agents.’ All agents are guided with skid-to-turn maneuvers. Therefore, on the roll channel roll angle is commanded as zero. Pitch and yaw channel commands differ for informed and naïve agents.

5.1 Informed Agent Guidance

Informed agent guidance has three different parts. By superposing these commands, the final command is created.

5.1.1 Velocity Pursuit Guidance Method

The velocity pursuit guidance method is one of the most popular guidance methods. The aim of the method is to change the direction of the munition velocity vector directly to the target. The application of this method is simple and useful. The angle difference between the velocity vector and missile to target vector goes through 0 after it is settled.

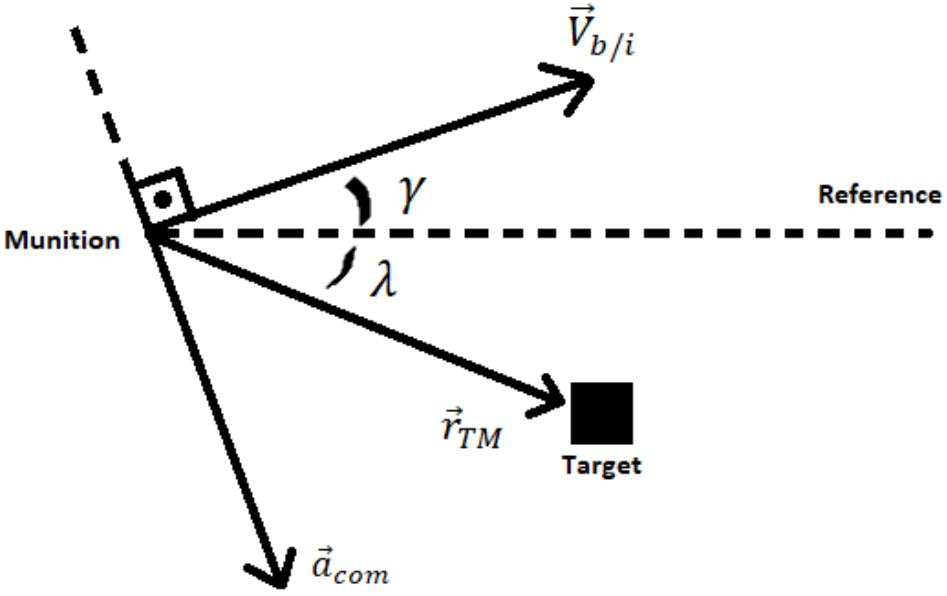

Figure 11 Velocity pursuit command scheme

$$\vec{\imath}_{TM}^{(i)} = \frac{\vec{r}_{TM}^{(i)}}{\left|\vec{r}_{TM}^{(i)}\right|} \tag{77}$$

$$\vec{\imath}_{V_m}^{(i)} = \frac{\vec{V}_{b/i}^{(i)}}{\left|\vec{V}_{b/i}^{(i)}\right|} \tag{78}$$

$$\vec{\omega}_{com}^{(i)} = \vec{\imath}_{TM}^{(i)} \times \vec{\imath}_{V_m}^{(i)} \tag{79}$$

$$\vec{a}_{com}^{(i)} = K\left(\vec{\omega}_{com}^{(i)} \times \vec{V}_{b/i}^{(i)}\right) \tag{80}$$

When this method is applied to a munition initially at (0,3000) and the target placed at (4000,0), the trajectory of the munition is expected, as shown in Figure 12.

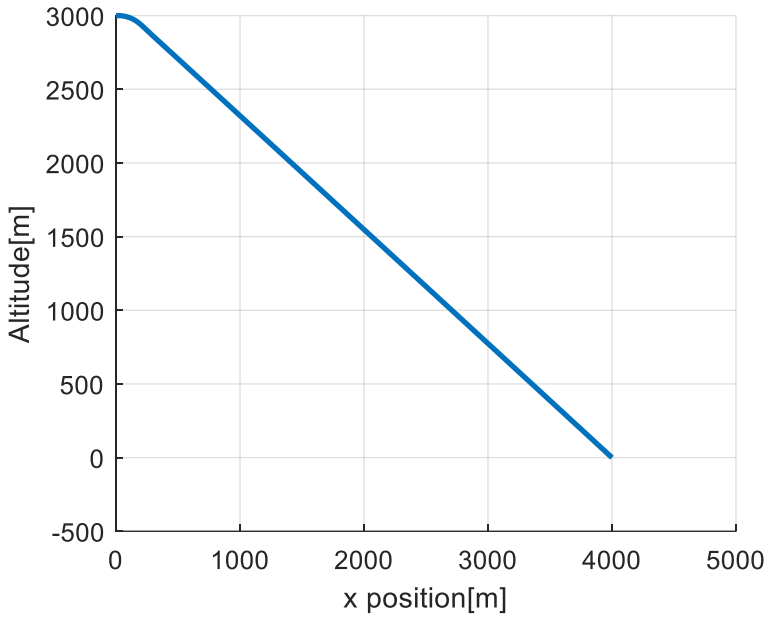

Figure 12 Trajectory example for velocity pursuit

5.1.2 Gravity Compensation

Since gravity is modeled in the system, the total command must be excluded from gravity. This will help us to give absolute acceleration commands. Gravity is modeled as not changing with altitude for this study.

$$\vec{a}_g{}^{(i)} = \begin{bmatrix} 0 \\ 0 \\ -g \end{bmatrix} \tag{81}$$

5.1.3 Collision Avoidance Command

Collision avoidance is provided by naïve agents but also informed agents create acceleration commands to avoid any collision. If any agent comes closer than the predefined distance at the y-axis of the inertial reference frame, the fixed acceleration command is applied as a collision avoidance command.

$$K_K = sign(distance_{closest}) \; and \; a_{col} > 0$$

$$\vec{a}_c{}^{(i)} = \begin{bmatrix} 0 \\ K_K a_{col} \\ 0 \end{bmatrix} \tag{82}$$

Where a_{col} is taken as $2\ m/s^2$ for the simulations.

5.1.4 Final Acceleration Command

The final acceleration command is created by superposing previously calculated commands explained before. These acceleration commands are summed at an inertial reference frame. After calculating the final acceleration command at the inertial reference frame, commands are transformed into the body reference frame and implemented by related autopilots.

$$\vec{a}^{(i)}_{final_{command}} = \vec{a}^{(i)}_{com} + \vec{a}_g{}^{(i)} + \vec{a}_c{}^{(i)} \tag{83}$$

$$\vec{a}^{(b)}_{final_{command}} = \hat{C}^{(b,i)}{}_{nav} \vec{a}^{(i)}_{final_{command}} \tag{84}$$

5.2 Naïve Agent Guidance

Naïve agent guidance has three separate parts. By superposing these commands, the final command is created.

5.2.1 Acceleration Command on Pitch Channel

Naïve agents are desired to follow the primary informed agents' current position at the pitch channel. The angle of the velocity vector at the pitch channel is called gamma (γ) pitch angle. Naïve agents' gamma pitch angle is commanded to look at the primary informed agent's current position. The primary informed agent is directly followed by the naïve agents at the pitch channel by applying this method. After implementation of this command, even if naïve agents are at a different altitude, they simply follow the vector between them and the primary informed agent and come together. Commanded angle is presented in Figure 13.

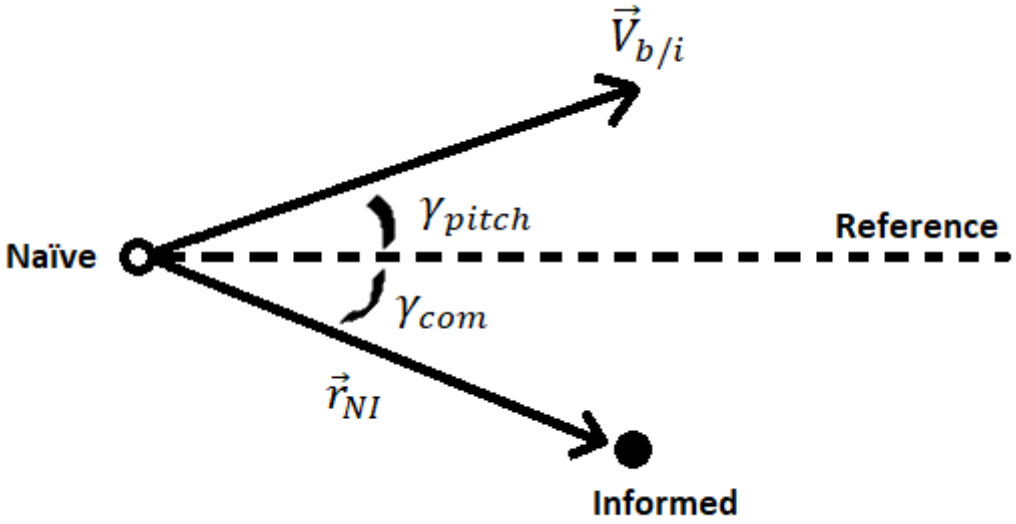

Figure 13 Naïve guidance on pitch channel scheme

$$\gamma_{com} = \arctan\left(\frac{\vec{r}_{NI}^{\,i}(3)}{\vec{r}_{NI}^{\,i}(1)}\right) \tag{85}$$

$$\gamma_{pitch} = \arctan\left(\frac{\vec{V}_{bi}^{\,i}(3)}{\vec{V}_{bi}^{\,i}(1)}\right) \tag{86}$$

$$\gamma_{error} = \gamma_{com} - \gamma_{pitch} \tag{87}$$

$$a_{z_{command}}^{(i)} = K_{\gamma}\,(\gamma_{error}) \tag{88}$$

K_{γ} is taken as 50, therefore for 1˚ angle error 0.8727 m/s^2 acceleration command is applied as a result.

5.2.2 Acceleration Command on Yaw Channel

Naïve agents are desired to move together collaboratively with the help of information of other agents' position data. Position tracker and potential function method are applied for this purpose. The desired horizontal position through the target is calculated using the potential function method. A position tracker is implemented to reach the desired position.

5.2.2.1 Potential function method

The potential function method is used to decide the horizontal position of an agent through the initial target direction. This method prevents agents from colliding or going away from each other. The potential function method is created as the agents can interact with a limited number of closest neighbors, and they also can interact with agents closer than a decided range. Effective neighbors are found after these limitations. The method is a summation of the effects of all effective neighbors for an agent. [29,30]

For positive constants a, b and c where a<b potential function is defined as:

$$J_{agent} = \sum_{i=1}^{n_{en}} \left[\frac{a}{2} \left| y_i - y_{agent} \right|^2 + \frac{bc}{2} e^{\left(-\frac{\left| y_i - y_{agent} \right|^2}{c} \right)} \right] \tag{89}$$

The potential function for a single agent with a=25, b=20, and c=10 can be plotted as shown in Figure 14.

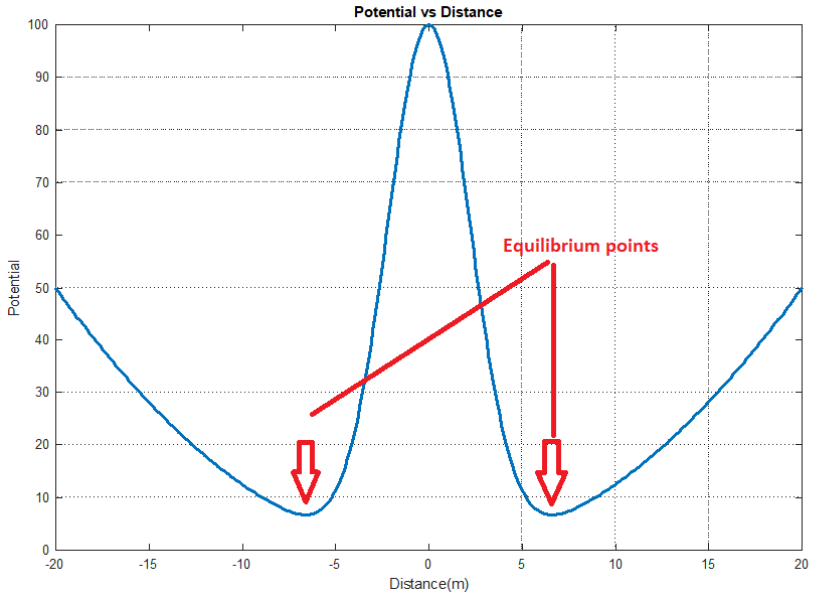

Figure 14 Potential function vs distance graph

The effect of one agent on another is calculated with nonlinear functions created before. Attraction and repulsion forces are superposed according to the position difference between agents. There are two equilibrium positions where attraction and repulsion forces cancel each other. For example, for distances larger than the equilibrium position, attraction forces are stronger, and for distances smaller than the equilibrium position, repulsion forces are stronger for a positive side.

For different distances d force on an agent is defined as:

$$F_{agent}(d) = -d\left(a - be^{\left(-\frac{|d|^2}{c} \right)} \right) \tag{90}$$

For a=25, b=20 and c=10 force function for a single agent can be plotted as shown in Figure 15.

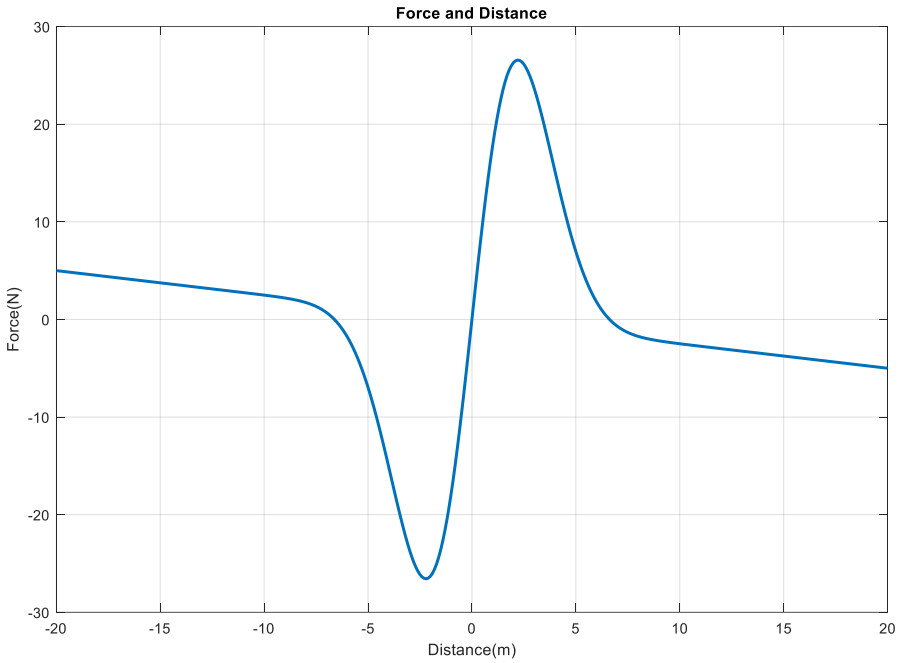

Figure 15 Force vs distance graph

The method calculates the resultant force of all effective neighbors on each agent at all steps. Then resultant force on an agent is integrated to find an equilibrium position for that agent. This application actively finds an appropriate position for agents to align for changing positions of others. All these calculations must be done according to the horizontal positions which is perpendicular to the initial target direction. Therefore, the desired horizontal position is also calculated through the initial target direction.

$$F_{Total} = \sum_{i=1}^{n_{en}} -d\left(a - be^{\left(-\frac{|d|^2}{c}\right)}\right) \tag{91}$$

$$y_{desired_{k+1}} = F_{Total}dt + y_{desired_k} \tag{92}$$

5.2.2.2 Position Controller

The position of an agent is needed to control to implement desired horizontal position calculated with the potential function method. To apply this method PD controller is used.

$$a_{y_{command}}^{(i)} = K_P(y_{desired} - y) + K_D \frac{d(y_{desired} - y)}{dt} \tag{93}$$

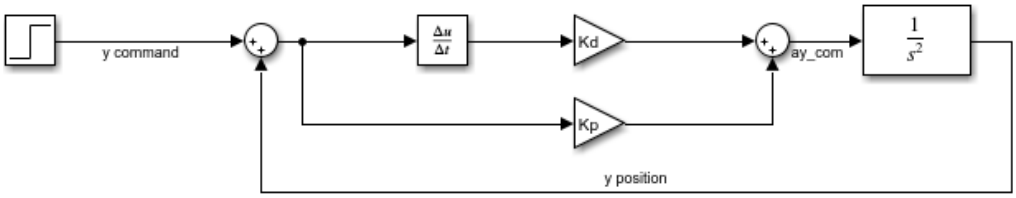

Figure 16 Position controller scheme

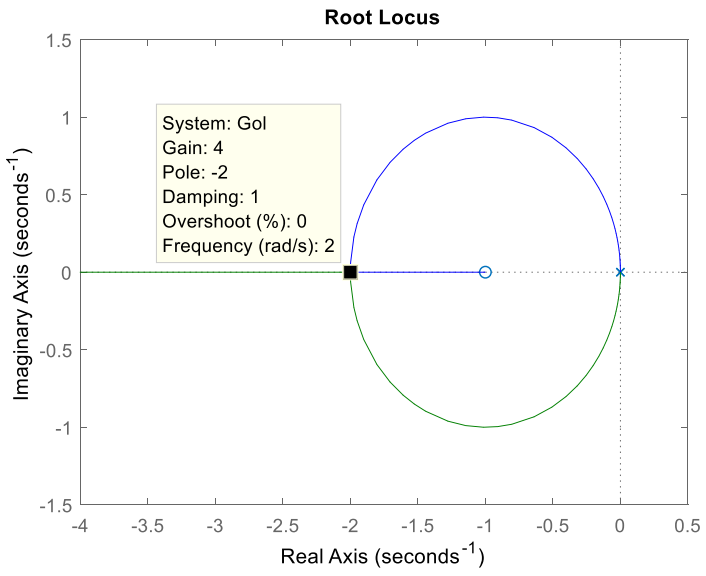

Figure 17 Position controller root locus

While designing close loop pole locations, the PD controller is designed with a zero placed at -1. Then gain is chosen as both poles are placed at -2. Therefore, Kp is selected as 4, and Kd is chosen as 4. Critically damped pole location is chosen for a controller design. Since there is zero closer to the imaginary axis, the step response has an overshoot although the poles are at the real axis.

Step response of the position controller can be seen in Figure 18.

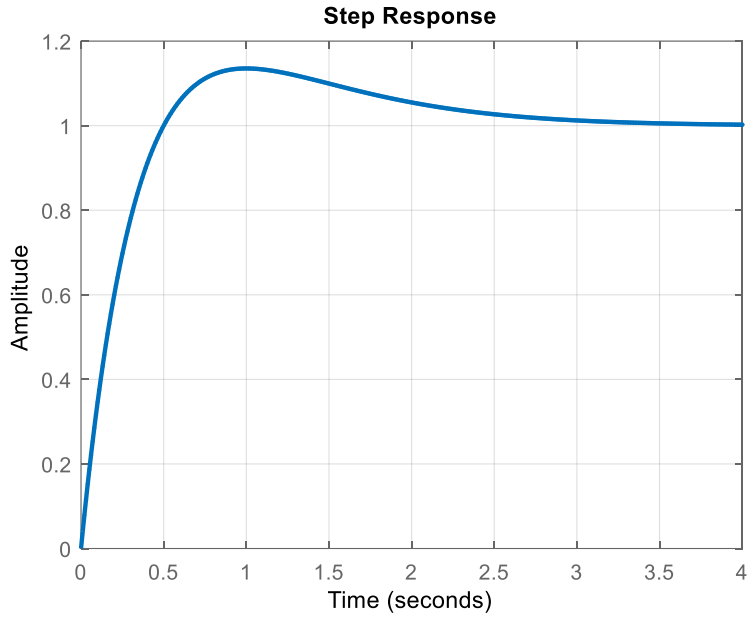

Figure 18 Position controller step response

5.2.3 Gravity Compensation

Since gravity is modeled in the system, the total command must be excluded from gravity. This will help us to give absolute acceleration commands. Gravity is modeled as not changing with altitude for this study.

$$\vec{a}_g{}^{(i)} = \begin{bmatrix} 0 \\ 0 \\ -g \end{bmatrix} \tag{94}$$

5.2.4 Final Acceleration Command

The final acceleration command is created by superposing previously calculated commands explained before. These acceleration commands are summed at an inertial reference frame. After calculating the final acceleration command at the inertial reference frame, commands are transformed into the body reference frame and implemented by related autopilots.

$$\vec{a}^{(i)}_{final_{command}} = \vec{a}^{(i)}_{z_{command}} + \vec{a}^{(i)}_{y_{command}} + \vec{a}_g{}^{(i)} \tag{95}$$

$$\vec{a}^{(b)}_{final_{command}} = \hat{C}^{(b,i)}{}_{nav}\vec{a}^{(i)}_{final_{command}} \tag{96}$$

CHAPTER 5

SIMULATION RESULTS

6.1 General Target-Munition Engagement for a Single Munition

In this study, munitions are thought of as gravity bombs. They do not have any propellers. Therefore, they are thrown with an initial velocity towards heading and accelerate with gravity and aerodynamic forces. Munitions are dropped from varying positions with the same velocities and accomplish the needed acceleration commands. The inertial reference frame is placed on the ground where the starting point of the central munition intersects the ground. Therefore, munition at the center starts from 0 at the x and y-axis, but the z-axis starts from negative of altitude.

On the other hand, a target is considered a non-moving object located at the heading of the munitions on the ground. Therefore, it has a large distance to the munitions at the x-axis of the inertial reference frame. Since there is a difference in altitude, it also has a considerable distance from the munitions at the z-axis. At the y-axis, a comparatively small difference is thought.

The single informed agent is placed at 4000 meters altitude from the ground with 0.3 Mach initial velocity. Target is located at 5000 meters in x direction on the ground. The munition is considered as informed about the target location. Munition changes its velocity vector's direction toward the target and meets with it by applying the velocity pursuit method explained before.

6.1.1 Rotational and Translational Position Outputs

The trajectory of the munition is shown in Figure 19.

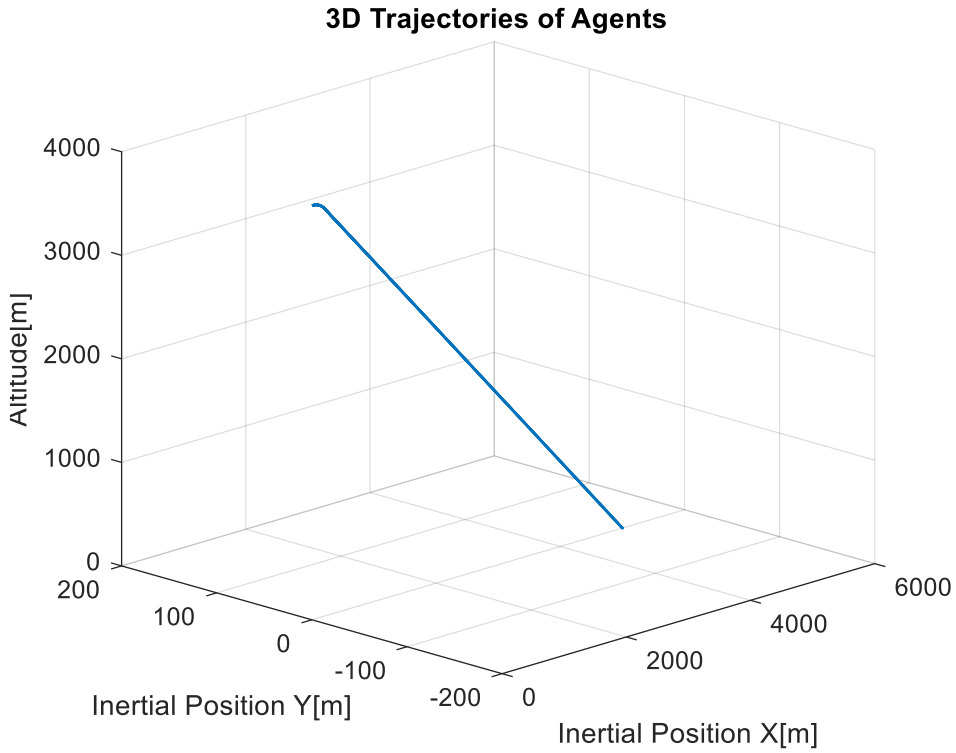

Figure 19 Trajectory of agent at scenario 0

The rolling angle is desired to stay around 0 during flight since the open-loop matrices for acceleration are created according to the non-rolling body assumption. STT autopilot design is chosen for all munitions. Other Euler angles change according to acceleration commands at the related motion channel.

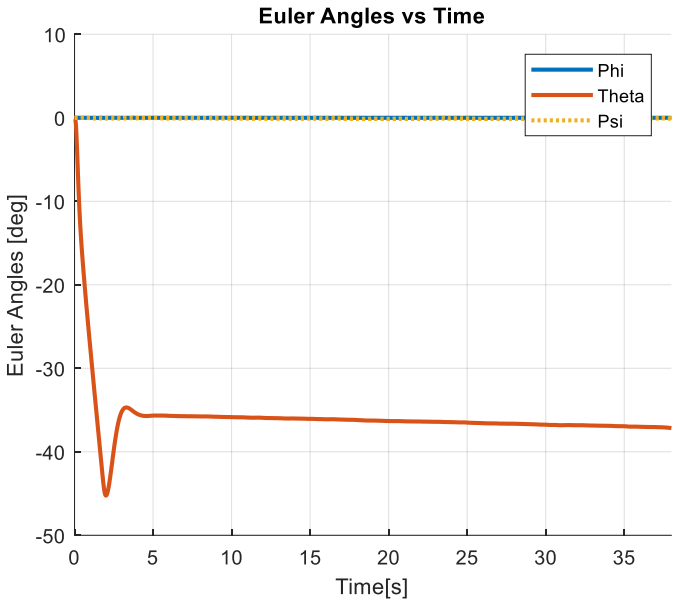

Figure 20 Euler angles of agent at scenario 0

6.1.2 Acceleration Commands and Related Outputs

Velocity pursuit guidance method commands for a single informed agent have been created according to target and munition positions all the time. These acceleration commands are followed with created autopilot outputs which are elevation, rudder, and aileron control surface angles. Acceleration commands and acceleration answers of autopilot are shown in Figure 21. Also, Inertial velocity components on the Inertial Reference Frame during a flight from releasing point(0,0,-4000m) to the final point(5000m,0,0) are shown.

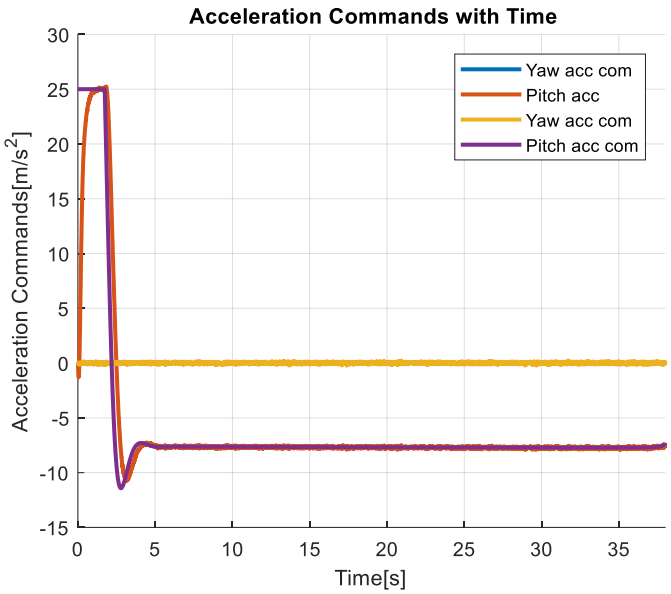

Figure 21 Acceleration commands of agent at scenario 0

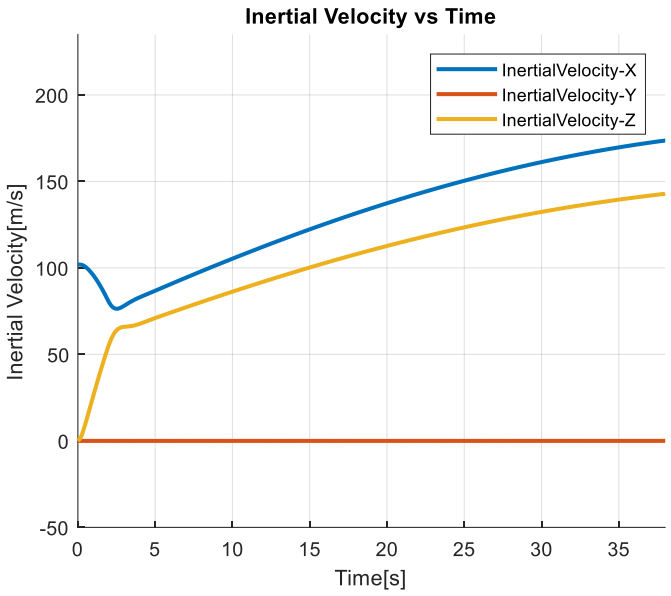

Figure 22 Inertial velocity components of agent at scenario 0

Application of these acceleration commands causes a change in the angle of attack and side slip angle of a munition. The change of these angles with an effect of aerodynamic parameters can be seen in Figure 21. The angle of attack α and side slip angle β are not so high and unrealistic. Therefore, an assumption of linear coefficients makes sense in this region [21].

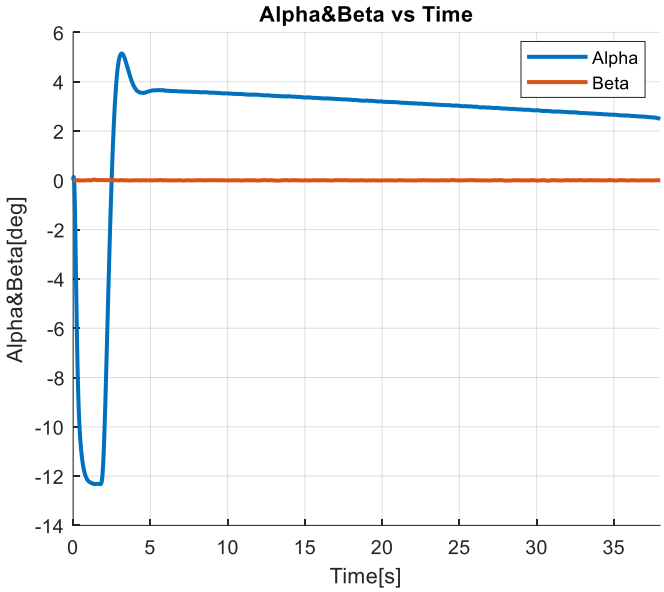

Figure 23 Alpha&Beta of agent at scenario 0

6.2 Informed and Naïve Agent Simulation Results

In this section, results for cooperative guidance and formation control algorithms will be explained. To apply this method, the swarm must have at least one informed and one naïve agent. Simulation outputs for informed and naïve agents are quite different from each other in many aspects. Also, there are outputs for a swarm related to uniformity and distribution. All these outputs will be investigated in this section. For potential functions used at the horizontal plane, the following parameters are applied. Effect distance at the horizontal axis for the potential function is named as d_{eff} and the limitation of attraction force distance is named as d_{af}.

Table 3 Potential function parameters

a=0.025
b=15
c=5
d_{eff}=60m
d_{af}=20m

6.2.1 First Scenario for a Munition Swarm

Swarm with one informed agent and nine naïve agents is concerned for the first scenario. The informed agent is released from 4000m altitude at 0 x and y positions at the inertial reference frame. Naïve agents are located at different horizontal locations between -24m and 21m and different altitudes between 3500m and 4500 m. Target is located at 5000m in the heading direction on the ground.

6.2.1.1 Informed Agent Results

Guidance commands are applied to meet with the target directly. Since the target is in the heading direction of the agent, it does not have a major acceleration command at the yaw axis, but because of the altitude difference between the target and munition release point, it applies comparatively large acceleration commands at the pitch axis of the body frame. Applied guidance commands can be seen in Figure 24.

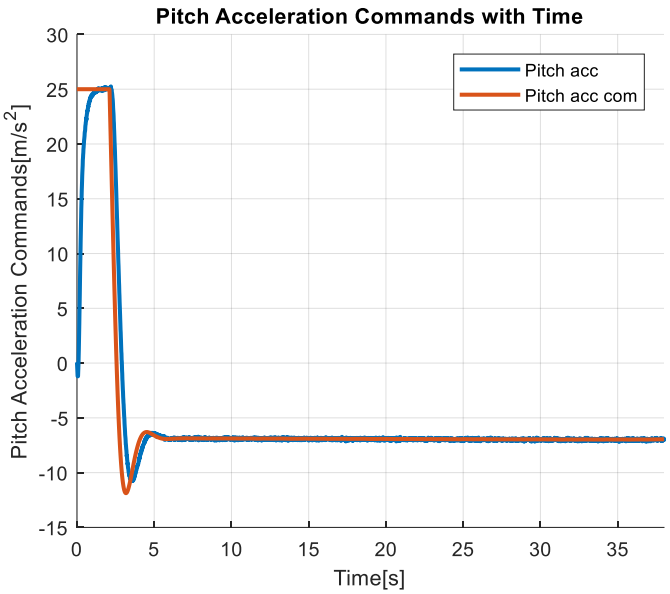

Figure 24 Pitch acceleration command-answer of informed agent at scenario 1

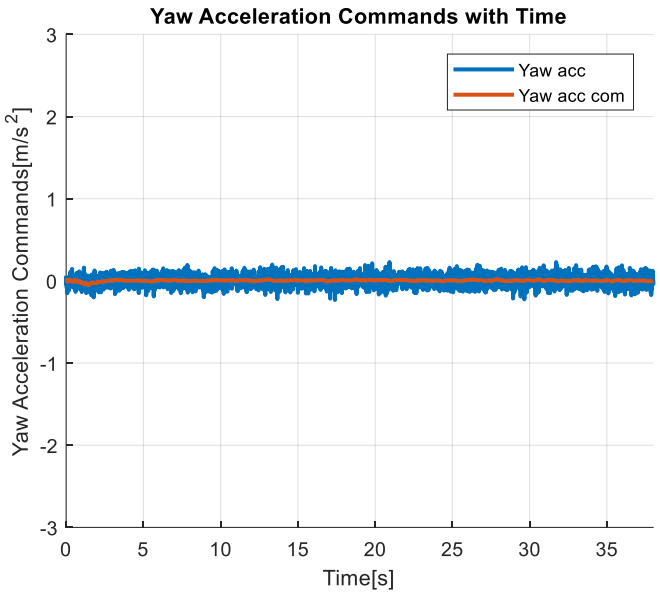

Figure 25 Yaw acceleration command-answer of informed agent at scenario 1

Again, since it is seen from the acceleration commands that the agent does not move at the horizontal plane of the inertial reference frame but dives at the vertical plane, as is seen from the figure.

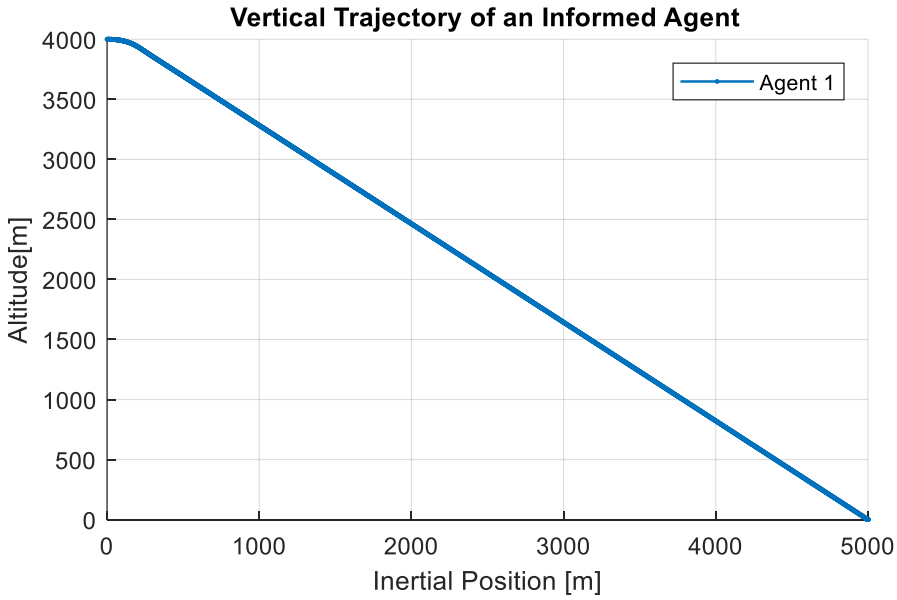

Figure 26 Vertical trajectory of an informed agent in scenario 1

6.2.1.2 Naïve Agent Results

Naïve agents follow the trajectory commanded by the potential function method at the horizontal plane. Low energy points are commanded with this method. The position controller applies the command at the yaw axis of the trajectory. Acceleration commands at the pitch axis are applied to follow the position of the informed agent. Therefore, similar trajectories at the vertical axis occurred even when altitude difference exists between different agents. The acceleration command shown in Figure 27 is applied for the 2nd agent of the swarm, which is one of the naïve agents.

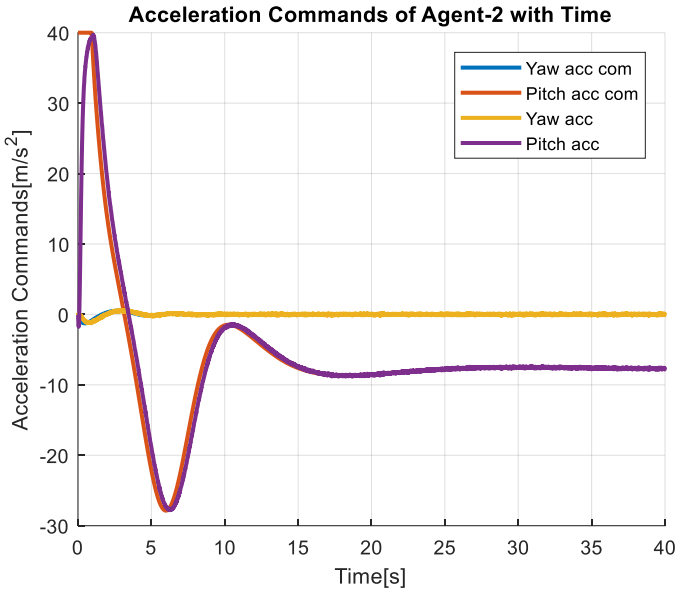

Figure 27 Acceleration commands of agent-2 for scenario 1

The result of the position decision algorithm based on the potential function method for the 2nd agent and its horizontal position can be seen in Figure 28.

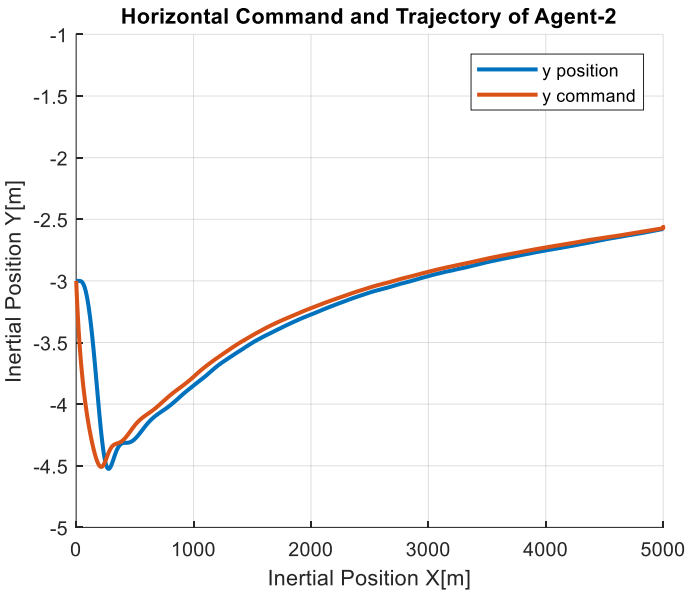

Figure 28 Horizontal command and trajectory of agent-2 for scenario 1

The horizontal position is followed successfully, and the command converges to some point at the end of the flight.

At the vertical plane, agent-2 follows the path shown by agent-1, which is an informed agent. As a result of this algorithm, naïve agents get close to the target at the same line of sight angle as the informed agent. The vertical trajectory of agent-2 and agent-1 are plotted together in Figure 29.

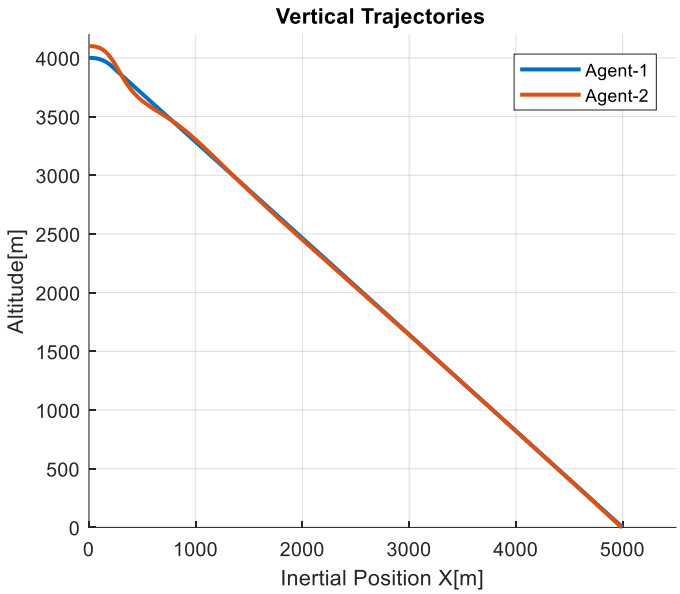

Figure 29 Vertical trajectory of agent-1 and 2 for scenario 1

6.2.1.3 Swarm Results

All the other naïve agents in the simulation apply commands similar to agent-2. According to their positions at the horizontal plane, they create horizontal position commands and follow the command. According to the relative position of the naïve agent to the informed agent, acceleration commands are applied to follow the informed agent at the pitch axis. As a result of this algorithm, all the agents move as a swarm and arrange their positions according to other agents and create the path shown in the figure.

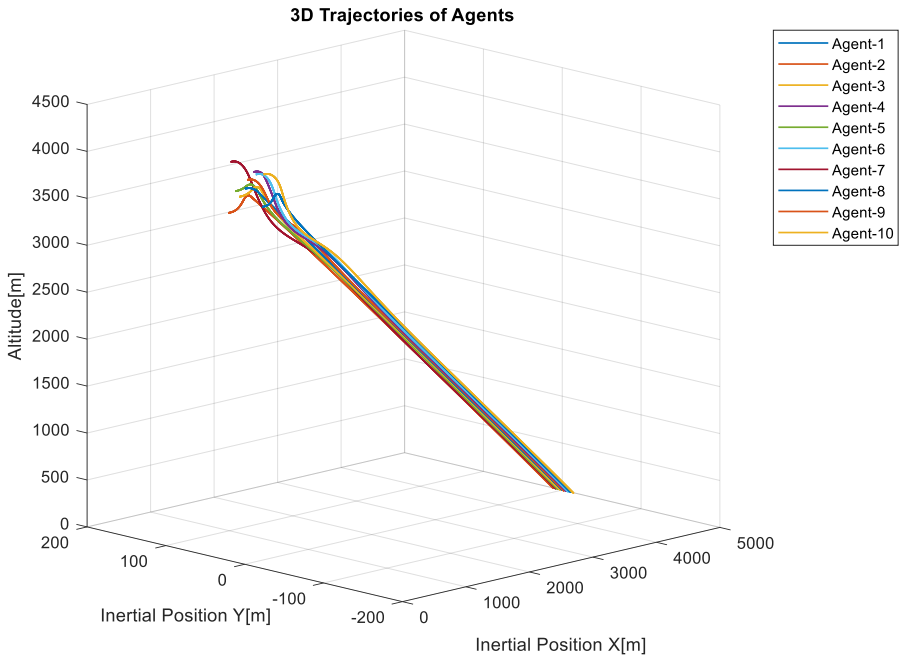

Figure 30 Trajectory of the swarm for scenario 1

The agents are released from different altitudes at the beginning. The acceleration commands at the pitch axis provide the swarm to close the target at the same pitch line of sight angle.

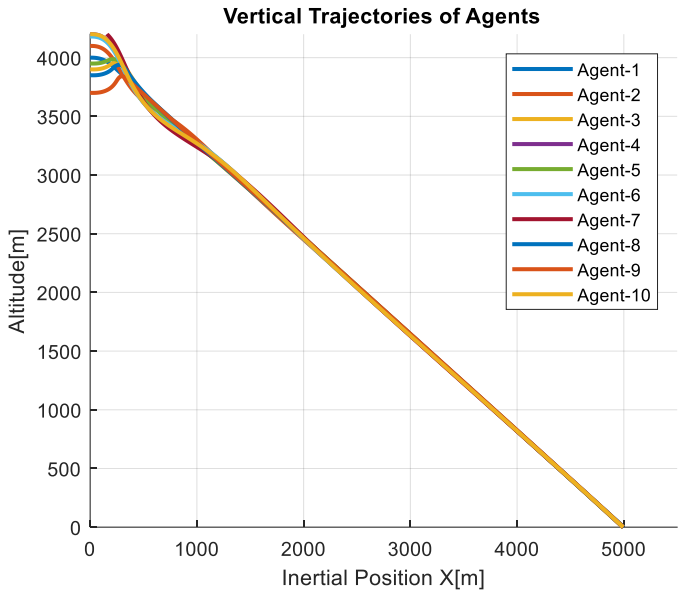

Figure 31 Vertical trajectory of the swarm for scenario 1

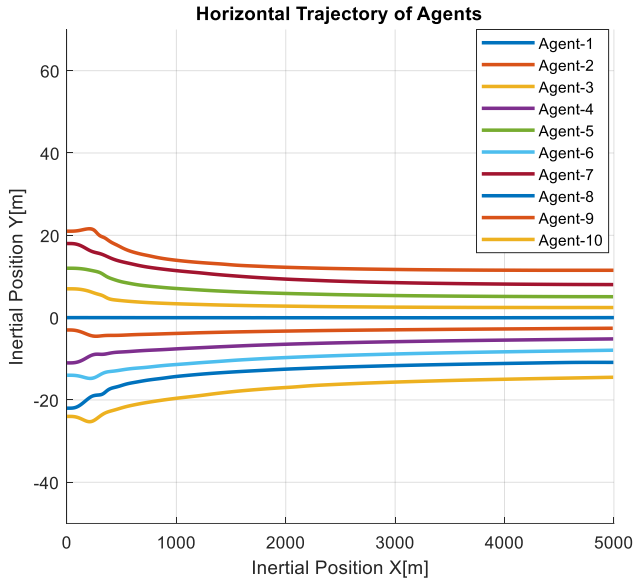

Figure 32 Horizontal trajectory of the swarm for scenario 1

Regulation on the horizontal plane is established with a potential function method on the y axis around the initial azimuth direction toward the target. A metric for irregularity is created to have an idea about uniformity. Irregularity is calculated with the Eq. (98).

The connection number is calculated by counting close neighbor connections. There are two close neighbor connections, one on the right side and one on the left side, for agents that are not at the rightmost or far leftmost on the horizontal plane. These two agents at the rightmost and leftmost have one close neighbor connection. Absolute value of distances for all connections are desired to be as close as possible for uniformity.

$$n_{con} = 2n_{agents} - 2 \tag{97}$$

$d_1 = |y_1 - y_2|$ if there is a close connection between agent-1 and agent-2.

$$\bar{d} = \frac{\sum_{i=1}^{n_{con}} d_i}{n_{con}}, \qquad L_{irr} = \frac{\sum_{i=1}^{n_{con}} |d_i - \bar{d}|}{n_{con}} \tag{98}$$

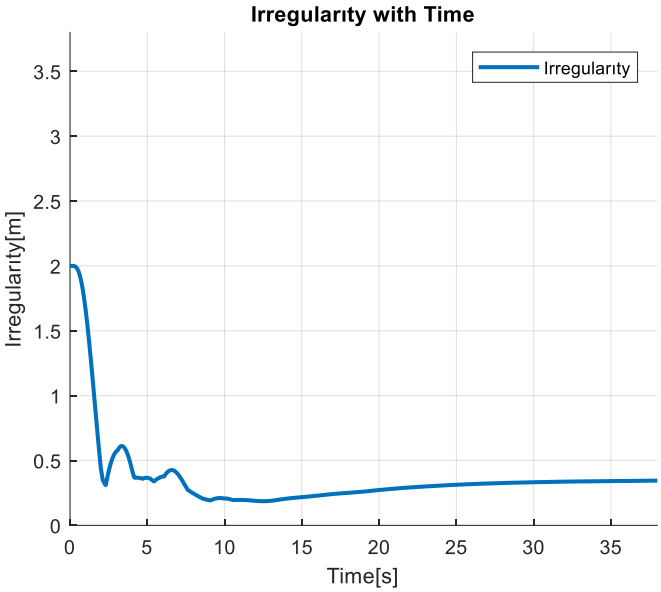

Figure 33 Irregularity of swarm for scenario 1

Irregularity decreases with time as a result of potential function applied at the horizontal plane. Position controller errors for each agent cause a little bit of irregularity for a swarm.

The average of the absolute values of the horizontal positions is called the wideness parameter to see how close the agents are. It is calculated as shown in the equation.

$$L_w = \frac{\sum_{i=1}^{n_{agents}} |y_i|}{n_{agents} - 1} \tag{99}$$

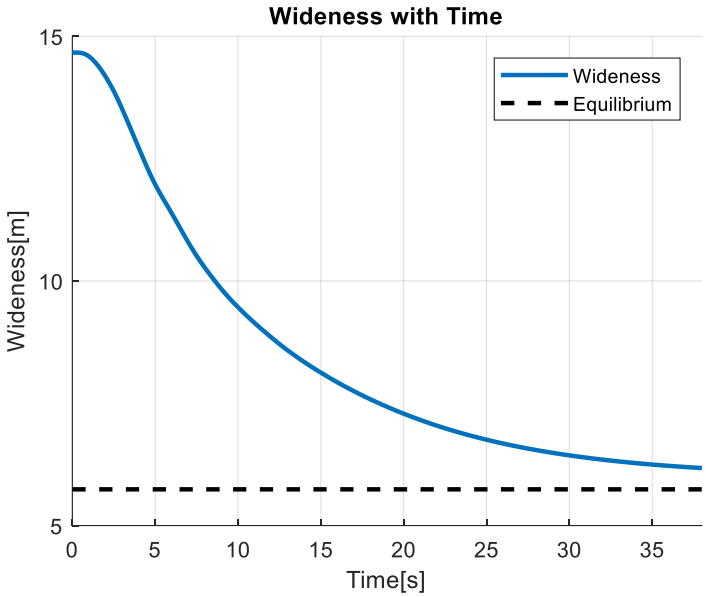

Figure 34 Wideness of swarm for scenario 1

The wideness of the swarm decreases with time because the initial conditions of the swarm are wider than the equilibrium distance of the potential function chosen.

The heading angle difference from an informed agent is calculated to check the heading angle error for the swarm. The parameter is found by taking the average of absolute Euler angle differences from agent-1 for naïve agents.

$$\psi_h = \frac{\sum_{i=1}^{(n_{agents}-1)} |\psi_i - \psi_1|}{n_{agents} - 1} \tag{99}$$

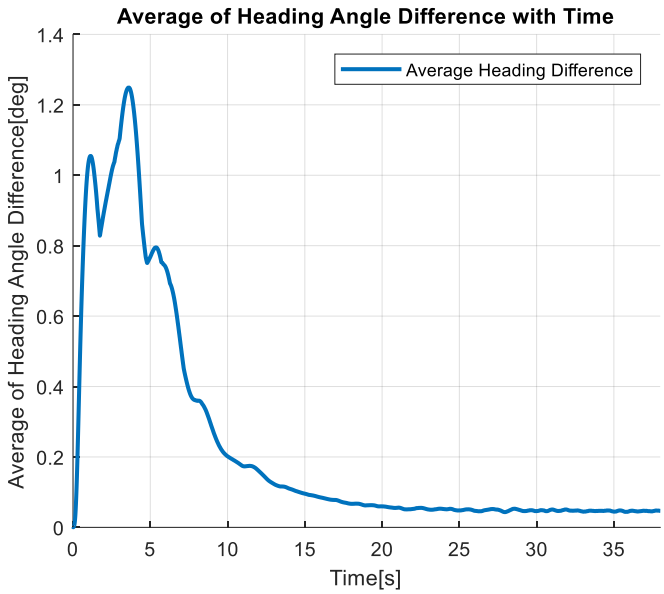

Figure 35 Average heading angle difference for scenario 1

The average heading angle difference from the informed agent starts from 0 since all the agents are released at the same initial heading angle. The average increases at first while the swarm is arranging itself at the horizontal plane. Then, it decreases with time and get closer to zero. A small amount of error stays because of irregularities in the swarm.

6.2.2 Second Scenario for a Munition Swarm

A swarm with one informed agent and six naïve agents is concerned for the second scenario. The informed agent is released from 4000m altitude at 0 x and y positions at the inertial reference frame. Naïve agents are located at different vertical locations between -22m and 18m and different altitudes between 3850m and 4250 m. Target is located at 5000m towards the heading direction and 250m on the left side of the heading direction on the ground. Potential function parameters are used the same with the scenario 1.

6.2.2.1 Informed Agent Results

The trajectory followed by an informed agent relies on the velocity pursuit guidance method applied between the release point and the target location. The informed agent directly changes its direction towards the target. This time the target is located 250m away from the nose direction initially. Therefore, the informed agent must apply acceleration commands in the y direction.

Applied guidance commands can be seen in Figure 36. Pitch commands are similar to the first scenario, but yaw commands differ from them.

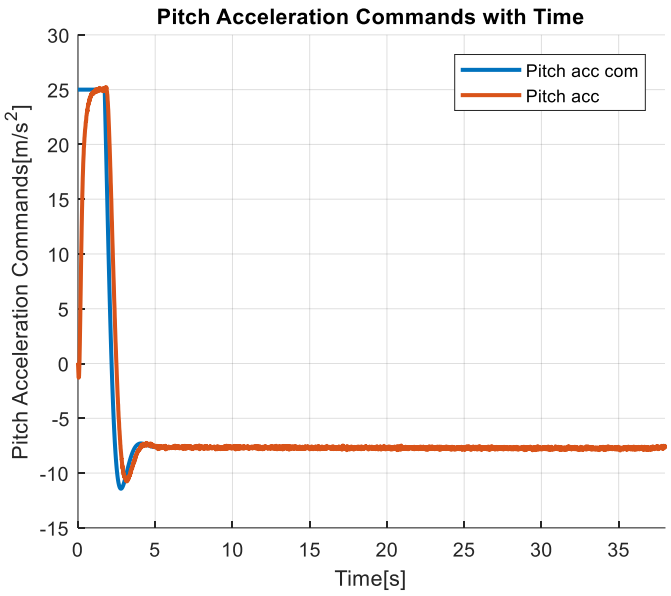

Figure 36 Pitch acceleration command-answer of informed agent for scenario 2

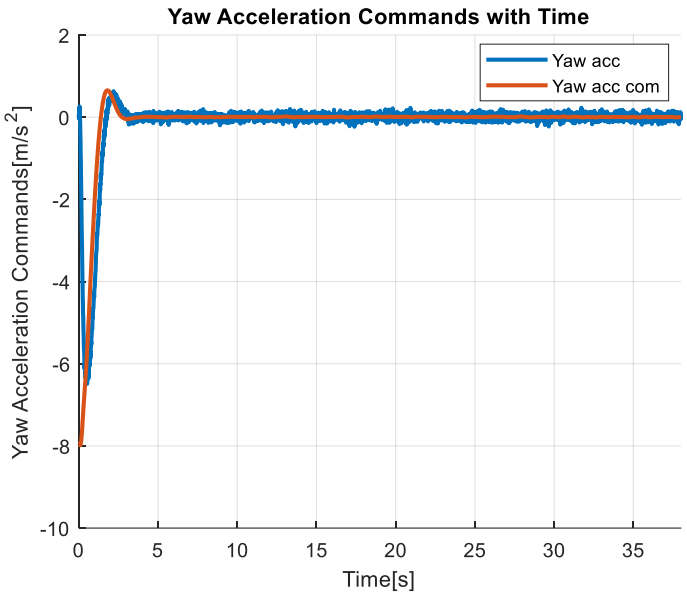

Figure 37 Yaw acceleration command-answer of informed agent for scenario 2

As it is seen from the acceleration commands, the informed agent applies acceleration commands on both channels to meet with the target this time. At the first times of flight, larger acceleration commands are applied and then they are settled around 0 for horizontal plane and around gravity for vertical plane. At the vertical plane, the agent starts its motion from 4000m altitude at 0 inertial x position and goes to 5000m inertial x position on the ground.

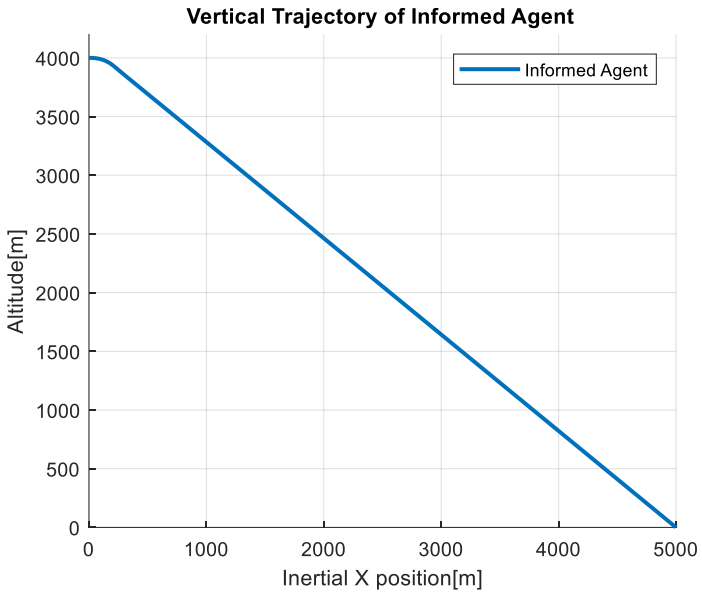

Figure 38 Vertical trajectory of informed agent for scenario 2

The agent moves along the negative y inertial direction as it moves at the positive x inertial direction to meet with the target, which is located at (5000m,-250m,0) position.

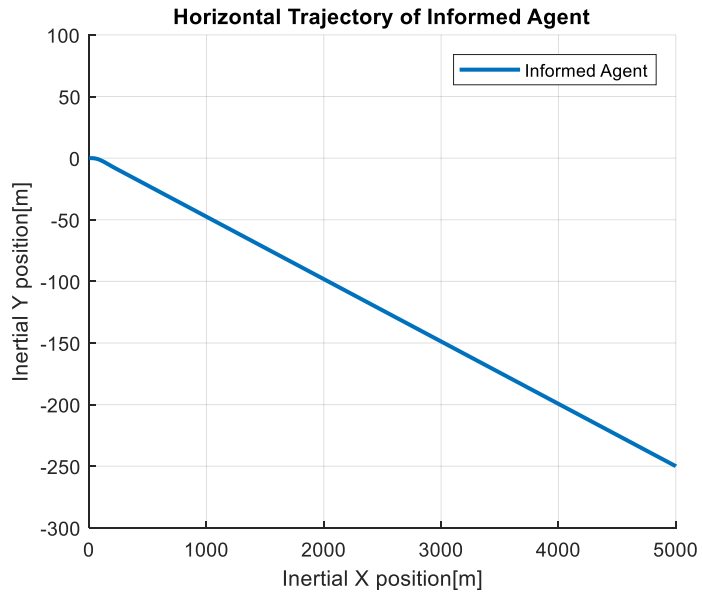

Figure 39 Horizontal trajectory of informed agent for scenario 2

6.2.2.2 Naïve Agent Results

The same acceleration command methods are applied for the 2nd scenario. This time, as a result of acceleration commands of an informed agent at the horizontal plane, naïve agents have to apply yaw acceleration commands. After some point, yaw acceleration commands converge around 0 because of the convergence of horizontal positions in the direction of motion.

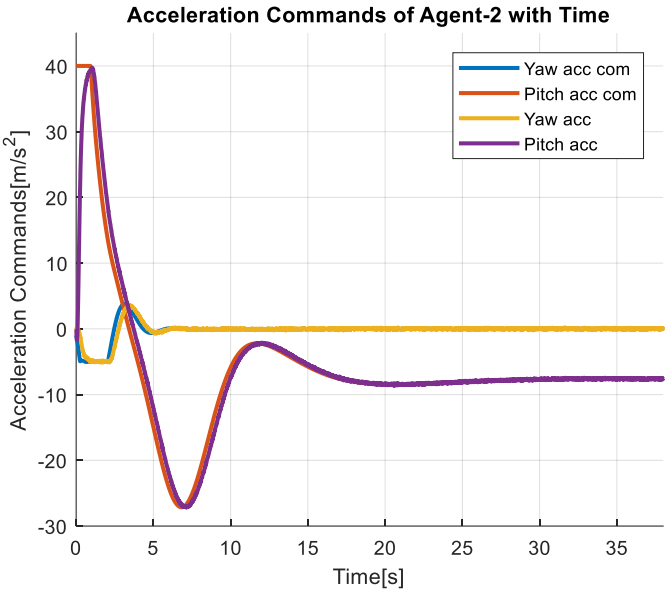

Figure 40 Acceleration commands and answers of agent-2 for scenario 2

The result of the position decision algorithm based on the potential function method for agent-2 and its horizontal position of it can be seen in Figure 41. The horizontal position is followed successfully by the controller on the horizontal plane.

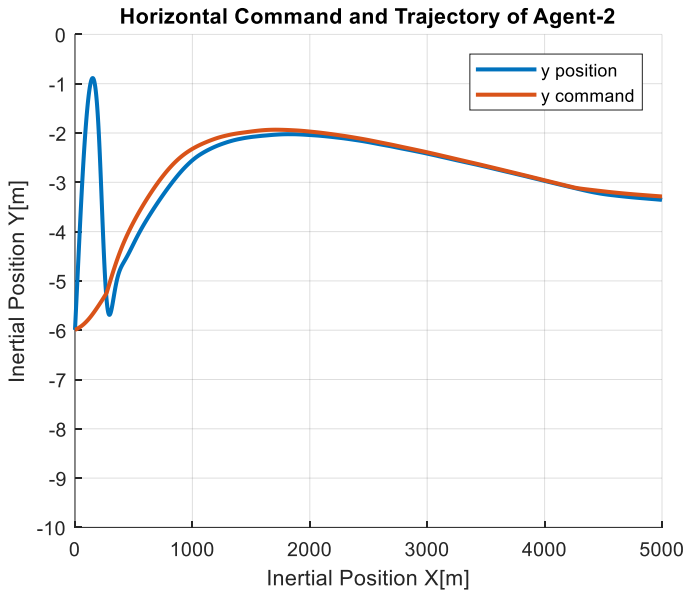

Figure 41 Horizontal command and trajectory of agent-2 for scenario 2

Agent-2 follows agent-1 on its own path toward the target on the horizontal plane near the agent-1. Since the informed agent (agent-1) moves on the y-axis of the inertial reference frame, the naïve agent moves alongside the informed agent toward the target with it.

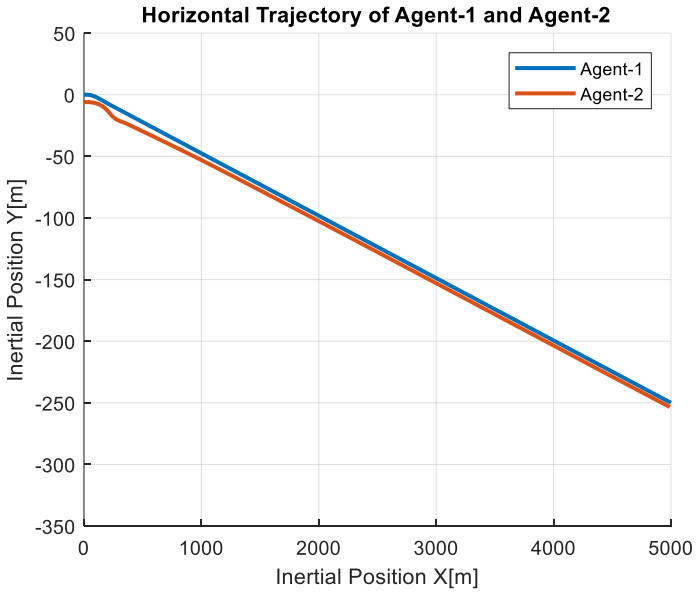

Figure 42 Horizontal trajectories of agent-1 and agent-2 for scenario 2

At the vertical plane, agent-2 follows the path shown by agent-1, which is an informed agent. As a result of applied method at the vertical plane, follows the path of informed agent.

The vertical trajectory of agent-2 and agent-1 are plotted together in Figure 43.

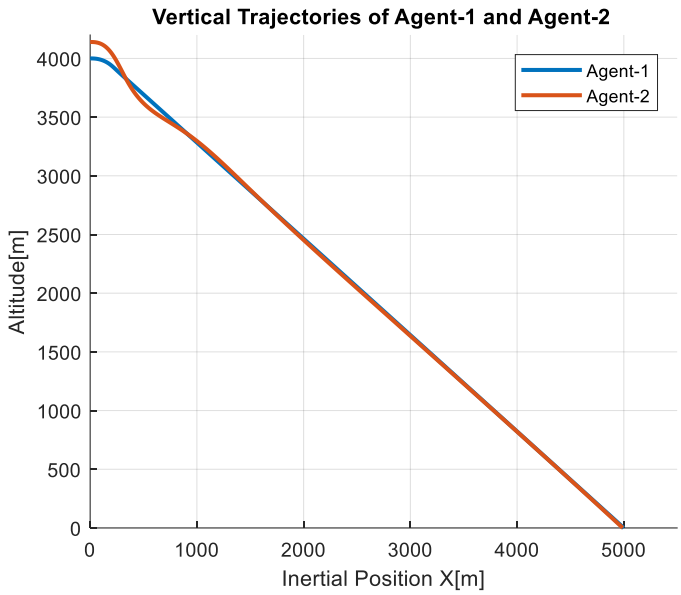

Figure 43 Vertical trajectories of agent-1 and agent-2 for scenario 2

6.2.2.3 Swarm Results

Informed agent and six naïve agents follow the path shown in figure 44. Agents arrange their vertical and horizontal position according to cooperative guidance method. Agents move in a uniformly distributed way toward the target position as it was for the first scenario.

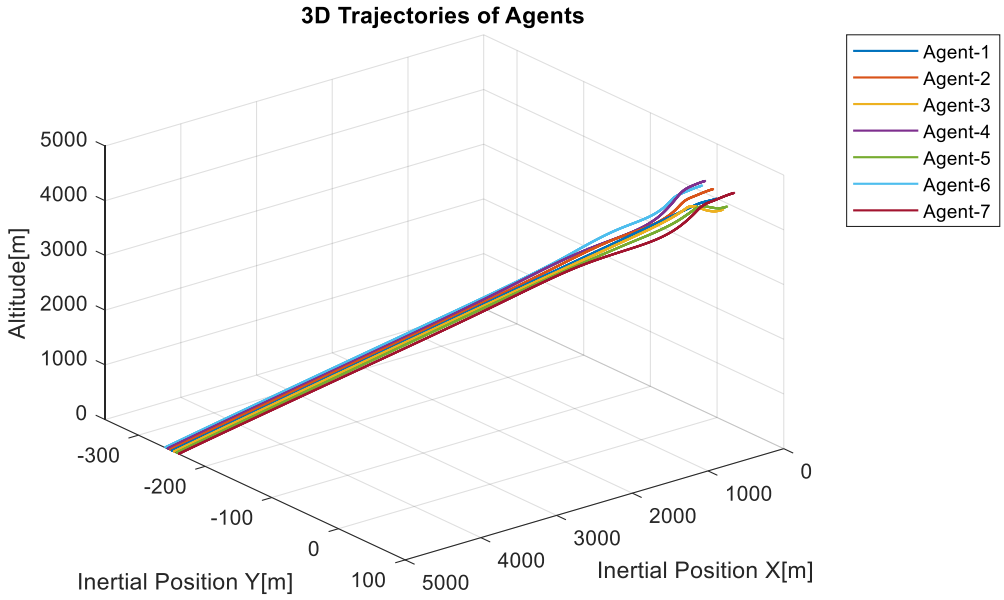

Figure 44 Trajectory of swarm for scenario 2

The figure is rotated to show the 3D trajectories more clearly. According to the Figure 44, agents start their motion from the right-upper side of the figure and the flight ends at the left-down side of the figure. The swarm moves with an informed agent at the y-axis of IRF. Trajectories at the horizontal and vertical planes are plotted in detail in Figure 45-46. On the vertical plane, agents tend to follow the LOS of the informed agent. On the horizontal plane, naïve agents position themselves according to the motion of informed agent at that plane.

Vertical trajectories are very similar to the first scenario, as it is seen in Figures 45 and 31. Although the agents start their motion from different altitudes the swarm follows the same line through the target.

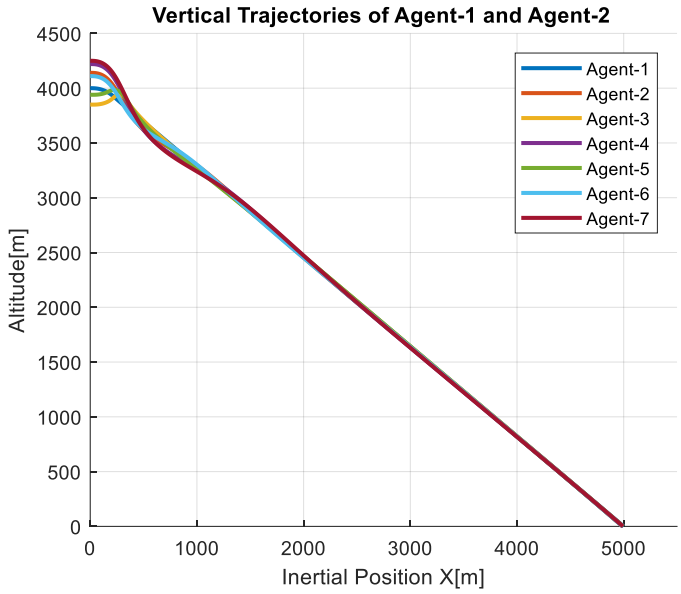

Figure 45 Vertical trajectory of swarm for scenario 2

Horizontal trajectories on the inertial frame can be plotted, as shown in Figure 46.

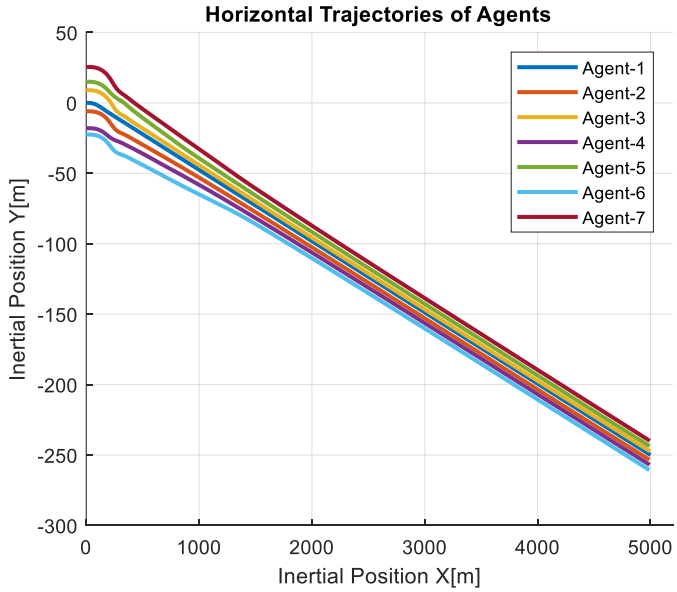

Figure 46 Horizontal trajectory of swarm for scenario 2

The irregularity metric is calculated as it is explained in the first scenario. Irregularity decreases over time, similar to the first scenario again. The irregularity increases at the beginning, and then it decreases. Swarm starts with more irregular configuration but at the final irregularity decreases converges around zero. When the informed agent changes its direction through the target at the beginning the irregularity increase but after some time the swarm agents arrange their position and irregularity decreases.

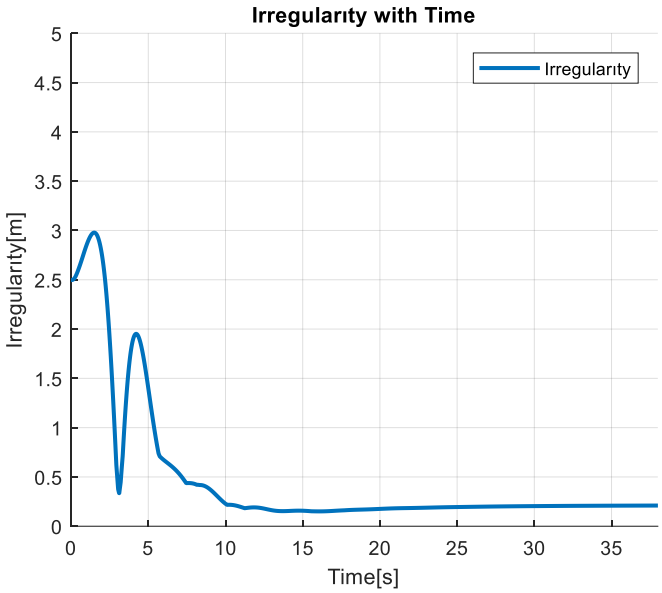

Figure 47 Irregularity of swarm for scenario 2

Agents are released from a wider initial condition than it was for the first scenario. Wideness decreases in time during the flight, as is seen from the Figure 48. Swarm wideness tends to go around equilibrium point of potential function.

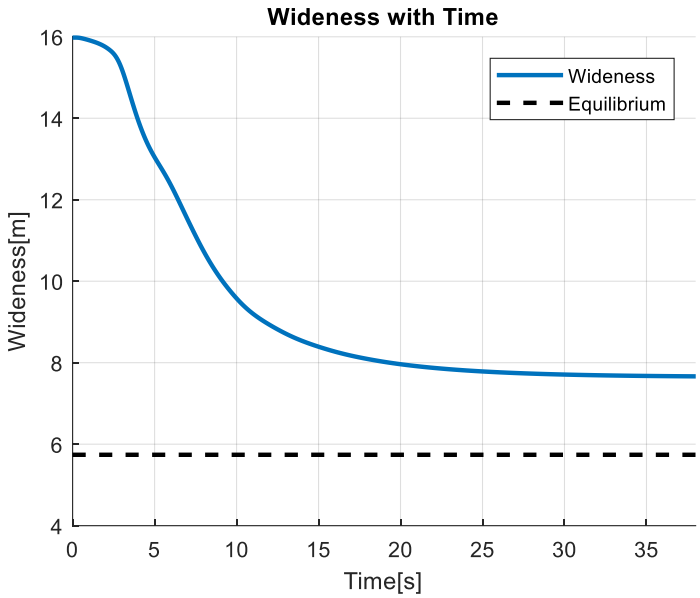

Figure 48 Wideness of swarm for scenario 2

Since the target is located with an angle to the heading angle, larger average heading angle differences are seen for scenario 2. At the beginning of the flight, the informed agent rotates its heading to the target and the difference increases; after some time, naïve agents follow the heading angle of the informed agent, and the heading angle difference decreases.

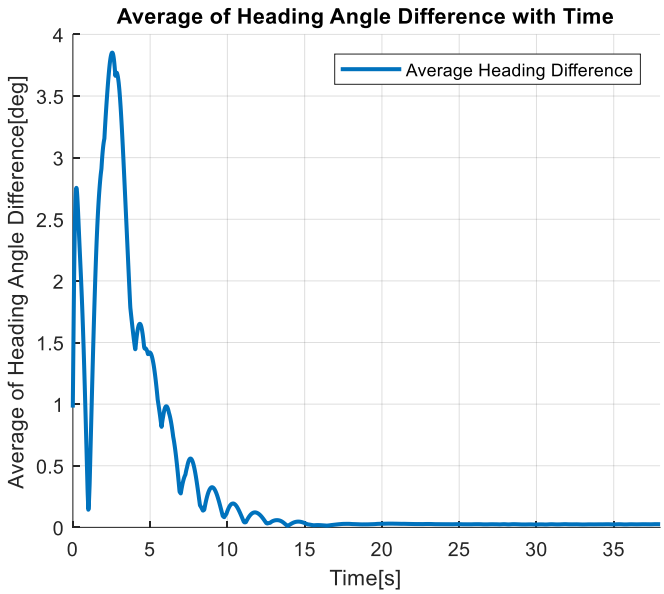

Figure 49 Average heading angle difference from informed agent for scenario 2

6.3 Effects of Informed Agent Number and Total Agent Number on Swarm

In this section, a defined scenario is simulated with different total agent numbers, and the results are investigated accordingly. In the second part, the same scenario is simulated for different numbers of informed agents. Potential function parameters are used the same as in scenario 1 for both parts.

6.3.1 Effect of Total Agent Number

First, a case of 5 total agents with one informed agent at the center is carried out. Then two new agents are added as one of them is placed 10 meters left of the leftmost agent, and the other is placed 10 meters right of the rightmost agent. New two agents are placed according to this logic each time up to 23 total agents.

Table 4 Initial horizontal positions case 1

Initial Inertial Y Position Agent 2=10	Initial Inertial Y Position Agent 3=-10
Initial Inertial Y Position Agent 4=20	Initial Inertial Y Position Agent 5=-20
Initial Inertial Y Position Agent 6=30	Initial Inertial Y Position Agent 7=-30
Initial Inertial Y Position Agent 8=40	Initial Inertial Y Position Agent 9=-40
Initial Inertial Y Position Agent 10=50	Initial Inertial Y Position Agent 11=-50
Initial Inertial Y Position Agent 12=60	Initial Inertial Y Position Agent 13=-60
Initial Inertial Y Position Agent 14=70	Initial Inertial Y Position Agent 15=-70
Initial Inertial Y Position Agent 16=80	Initial Inertial Y Position Agent 17=-80
Initial Inertial Y Position Agent 18=90	Initial Inertial Y Position Agent 19=-90
Initial Inertial Y Position Agent 20=100	Initial Inertial Y Position Agent 21=-100
Initial Inertial Y Position Agent 22=110	Initial Inertial Y Position Agent 23=-110

The informed agent is released from 4000m altitude at 0 x and y positions at the inertial reference frame. Naïve agents are located at different horizontal locations, shown in Table 4, at the same altitude. The same altitude is chosen for all agents to eliminate the effects of altitude difference, and new agents are placed at equal distances to eliminate the irregularity difference effect of initial conditions when new agents are added. Target is located at 5000m towards the heading direction and 200m on the left side of the heading direction on the ground.

Wideness results for various number of agents is shown in the figure. As we add agents to the swarm, initial wideness starts from a higher value. For all the cases, swarm tends to come closer to each other during flight because of the equilibrium point of the potential function. The equilibrium point for the two agents is 5.7 for the parameters given in Table 3.

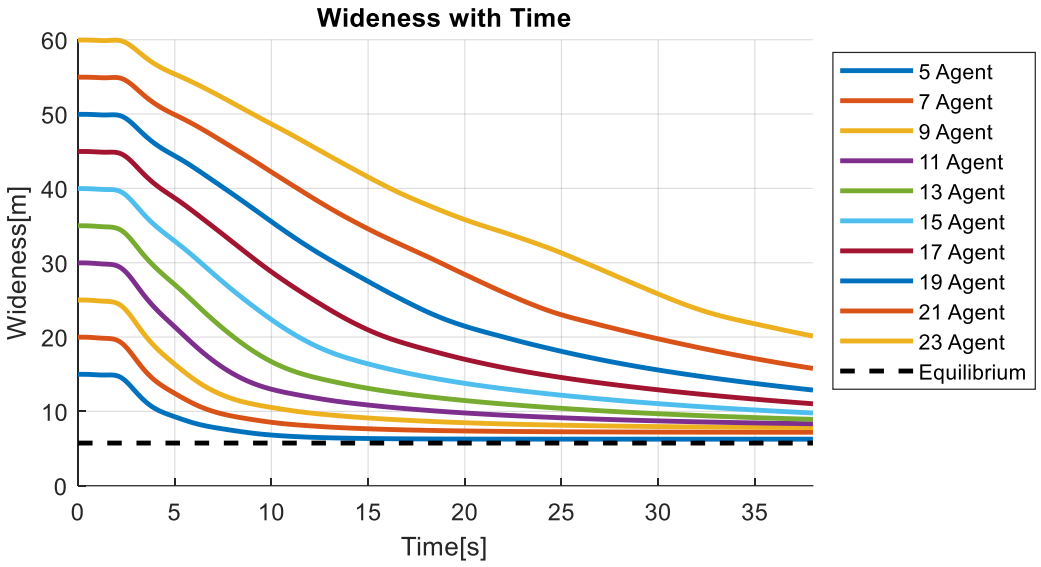

Figure 50 Wideness for various number of agents

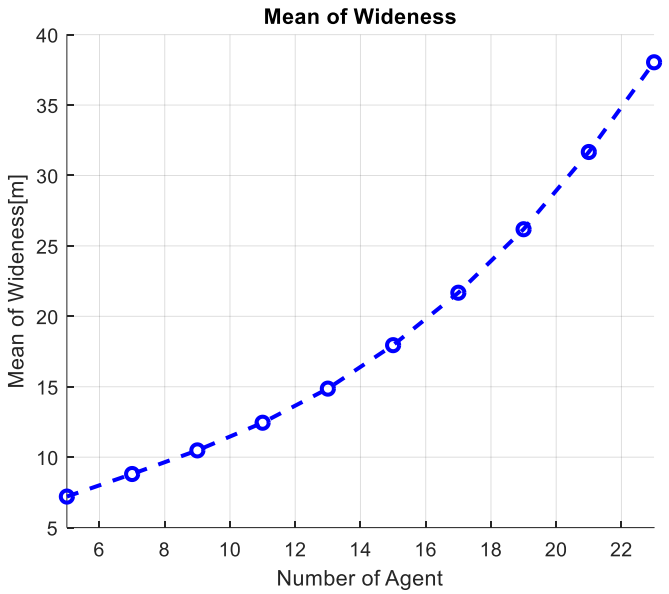

Figure 51 Mean of wideness vs. number of agents.

The mean of wideness value increases when we add new agents to the system as expected. New agents placed at the outside increase the wideness since they do not pass the inner agents of the swarm. They follow a path closer to the inner agent to them according to the potential function horizontal position command.

Irregularity with time for various informed agent numbers is plotted at Figure 52. Since the agents start from regular horizontal configuration, irregularity value starts from zero. In all cases, the informed agent makes a turn toward the target and changes its heading to the target at the first times of the flight. As a result, irregularity increases while the agents are trying to arrange their positions and heading angles according to informed agent. Then irregularity tends to decrease with time for all cases with the help of potential function method. A decrease in irregularity takes more time when there are a greater number of agents.

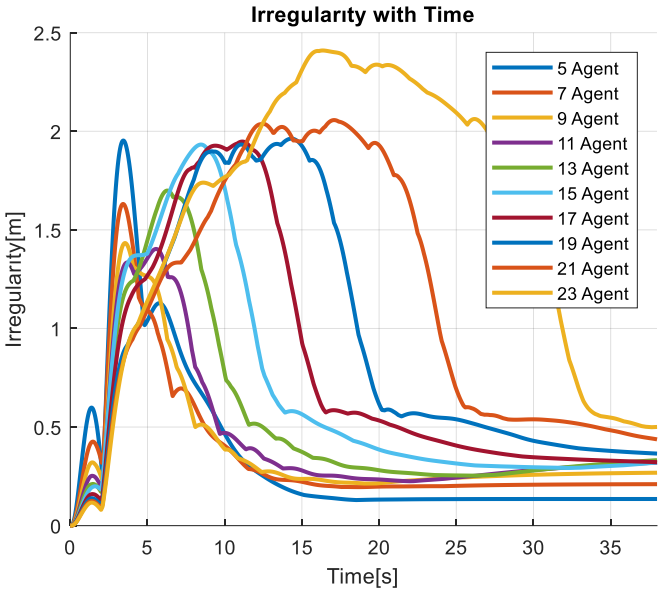

Figure 52 Irregularity for various number of agents

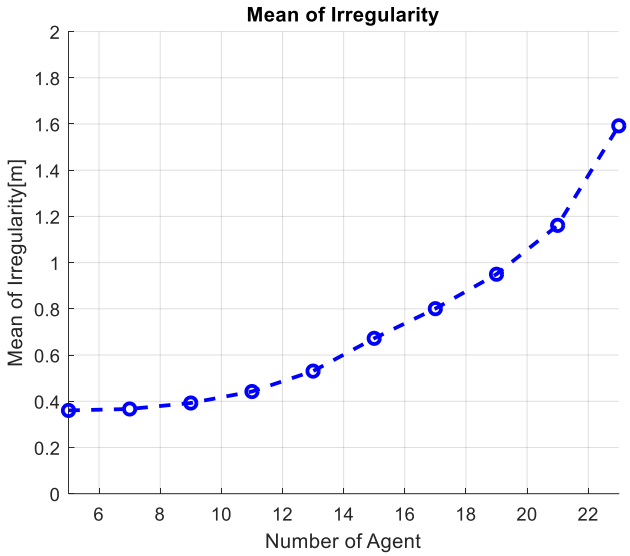

Figure 53 Mean of irregularity vs. number of agents

The mean of irregularity increases with the number of agents, as it is expected from Figure 50. It takes more time to transform to a more regular configuration at the horizontal axis since there are more agents that affect each other and more connections to handle.

The average heading difference from agent-1 with time is shown in Figure 54 for changing number of total agents.

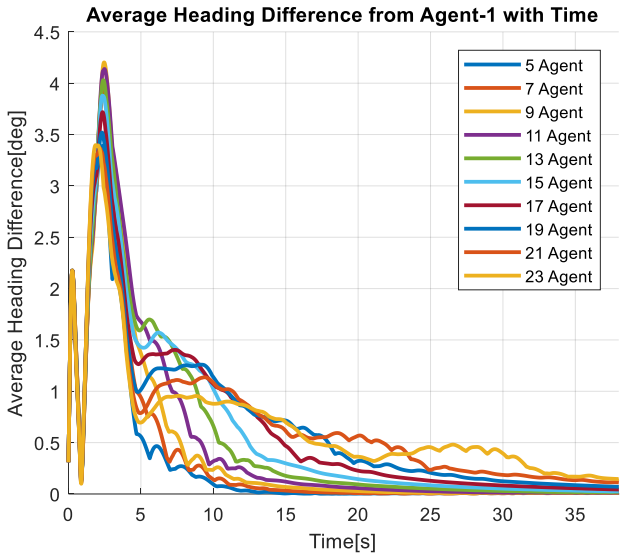

Figure 54 Average heading difference from agent-1 for various agent numbers

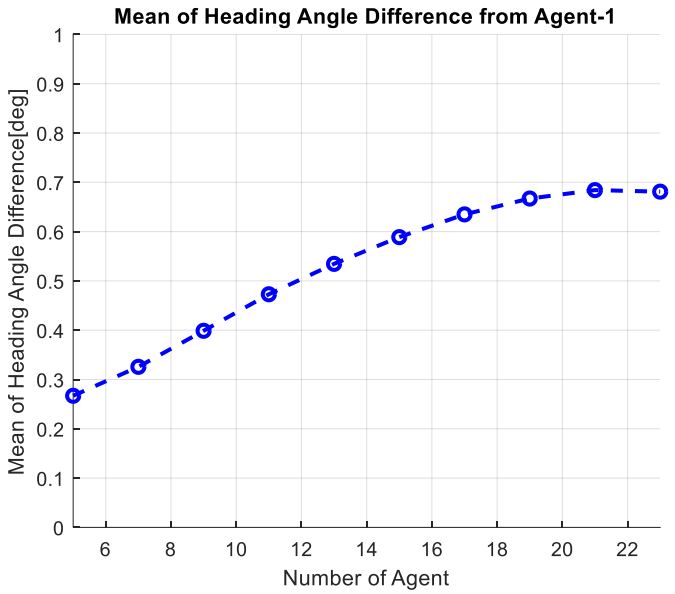

Figure 55 Mean of heading angle difference from agent-1 vs. number of agents

As it is seen in Figure 54, it is easier for the swarm to align the heading angle with the informed agent when there are fewer agents. This is because there are more agents to configure their positions. Attraction and repulsion forces between agents settle at some point where all the agents come to an equilibrium configuration, and since there are more agents, there are more forces that affect each other. All these forces change the heading angles of the munitions during flight while they are positioning themselves to a more uniform configuration. It takes again more time to arrange when there are more agents to organize.

6.3.2 Effect of Informed Agent Number

In this part, 23 agents are released from random y positions between -55 to 55 meters from the center. Agents follow a uniformly distributed trajectory and meet with a target. The final positions of this run are saved and used for informed agents as a target command. Simulations are completed for a different number of informed agents. The effect of informed agent numbers on irregularity, wideness, and heading errors are investigated.

Table 5 Initial horizontal positions case 2

Initial Inertial Y Position Agent 2=-4	Initial Inertial Y Position Agent 3=6
Initial Inertial Y Position Agent 4=-12	Initial Inertial Y Position Agent 5=10
Initial Inertial Y Position Agent 6=-15	Initial Inertial Y Position Agent 7=17
Initial Inertial Y Position Agent 8=-22	Initial Inertial Y Position Agent 9=21
Initial Inertial Y Position Agent 10=-24	Initial Inertial Y Position Agent 11=23
Initial Inertial Y Position Agent 12=-29	Initial Inertial Y Position Agent 13=30
Initial Inertial Y Position Agent 14=-32	Initial Inertial Y Position Agent 15=35
Initial Inertial Y Position Agent 16=-42	Initial Inertial Y Position Agent 17=41
Initial Inertial Y Position Agent 18=-44	Initial Inertial Y Position Agent 19=44
Initial Inertial Y Position Agent 20=-48	Initial Inertial Y Position Agent 21=48
Initial Inertial Y Position Agent 22=-55	Initial Inertial Y Position Agent 23=55

The informed agent is released from 4000m altitude at 0 x and y positions at the inertial reference frame. Naïve agents are located at the horizontal locations shown in Table 5 at the same altitude. Agents start from various distances from each other, but they arrange their positions during the flight. Irregularity decreases with the application of the potential function.

The same altitude is chosen for all agents to eliminate the effects of altitude difference. Target is located at 5000m towards the heading direction and 200m on the left side of the heading direction on the ground.

Wideness for various informed agents with 23 total agents is shown in Figure 54, and the mean of wideness values during flight for different runs are also shown. All runs start with the same wideness since the initial conditions are the same for all runs.

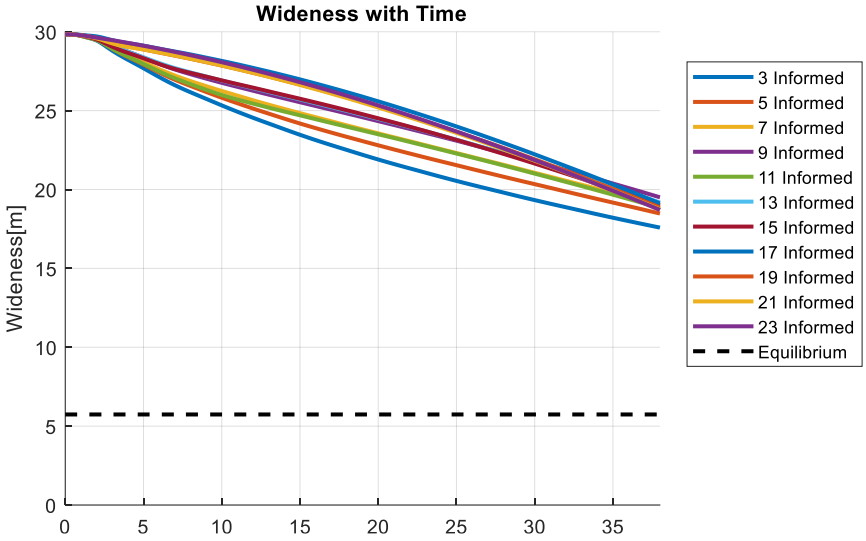

Figure 56 Wideness for various number of informed agents

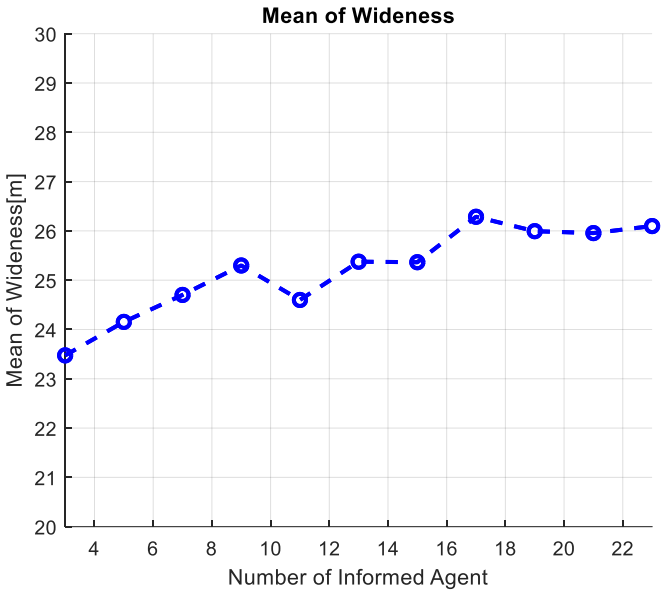

Figure 55 Mean of wideness vs. number of informed agents

Number of informed agents affect the trajectory of all agents because the potential function method uses neighbors' positions while computing equilibrium points for naïve agents. Therefore, the wideness of the agents also differs for the number of informed agents in the swarm. According to potential function parameters, the equilibrium distance is smaller than the initial distances. Naïve agents tend to come closer and distribute themselves uniformly. For all the cases, swarm agents come

closer to each other while they approach the target. Swarm tends to move closer to each other a little when the number of informed agents is decreased for the same total number of agents as a result of potential function application.

Irregularity with time for various informed agent numbers is plotted in Figure 57. All runs start with the same irregularity since the initial conditions are the same for all.

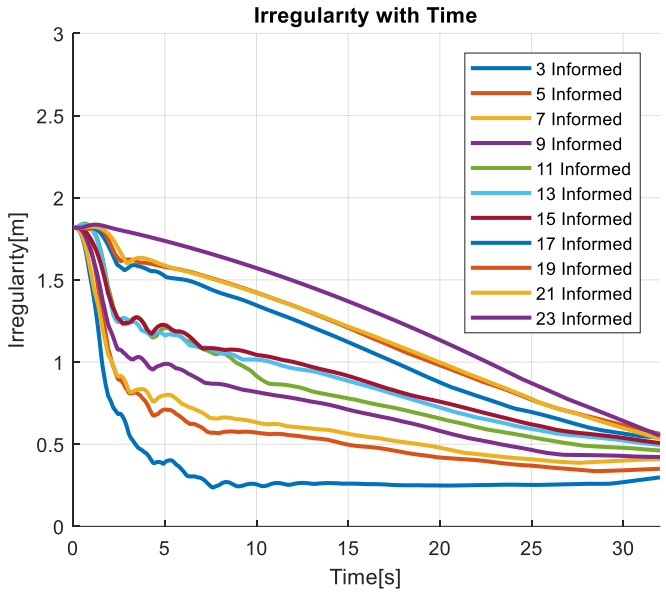

Figure 57 Irregularity for various number of informed agents

The mean values of irregularity for different runs are compared in Figure 58. Mean is calculated according to time for all.

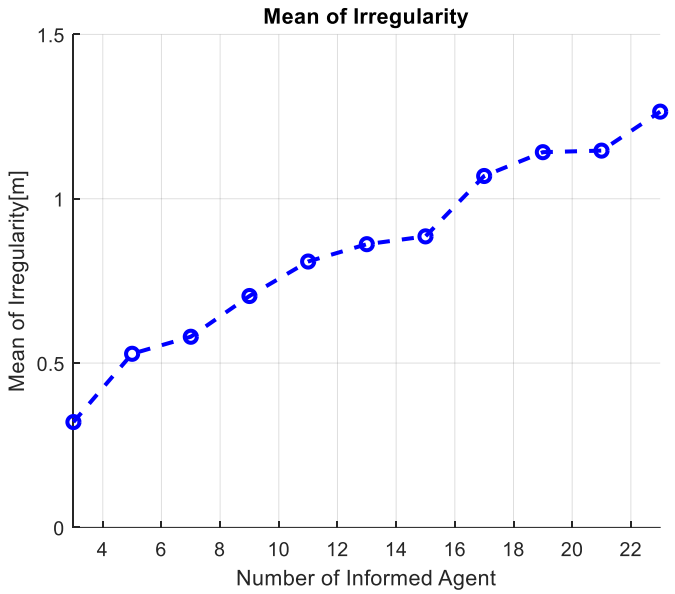

Figure 58 Mean of irregularity vs. number of informed agents

Irregularity for all runs starts from the same point, similar to a wideness, as explained before. Irregularity of the swarm decreases with time for all conditions, even if all agents are informed. Because informed agents are commanded to go relatively regular positions at the final when it is compared with release positions. It is clearly seen that as the number of informed agents decreases, the system converges faster to a more regular configuration. This is simply because the primary mission of naïve agents is to provide a uniform and safe flight on the horizontal plane. According to these plots, even when all agents are informed and go to a uniform final configuration, they fly in a more irregular configuration.

The average heading errors from agent-1 with time for different runs are plotted together in Figure 58.

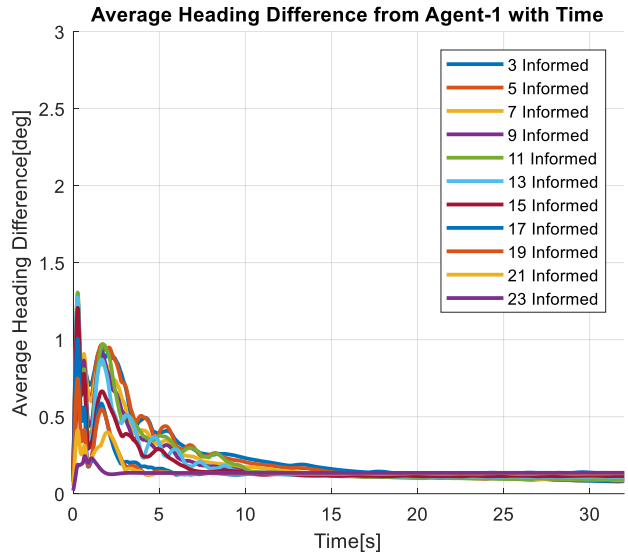

Figure 58 Average heading difference from agent-1 for various number of informed agents

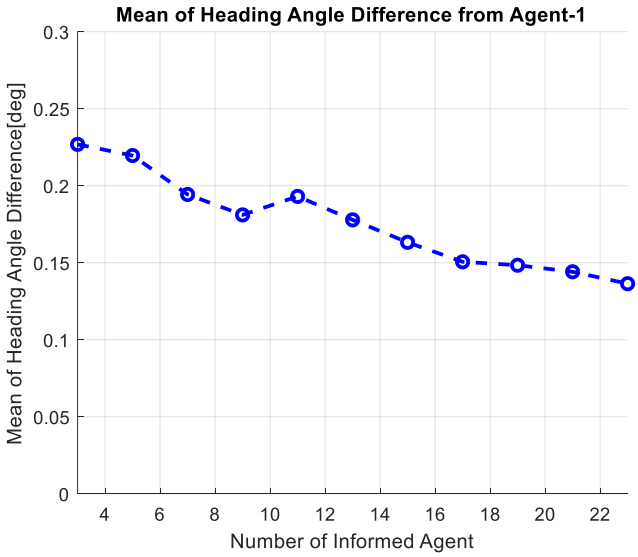

Figure 59 Mean of heading angle difference vs. number of informed agents

The average heading angle error from agent-1 decreases when the informed agent number is increased according to the results. This is because informed agents correct their own heading angle using the target information which they use to create acceleration commands. Furthermore, by correcting their own heading angle, they also shape the trajectory of the neighbor agents even if they are naïve agents. As a result, this helps to correct the heading angle of the swarm overall much faster.

CONCLUSION

In this thesis study, a cooperative guidance method with a formation controller for a guided munition swarm is proposed. This munition swarm consists of informed and naïve agents, which are gravity bombs that don't have any propeller. A Radiofrequency data link is considered as a data transfer mechanism for the swarm. It is observed from nature that even the communication and collaboration of small animals can accomplish extreme duties. The power of integrity makes the goals achievable, which are quite hard for an individual. Starting from this point of view, communication can be used for a munition swarm to achieve important goals.

Swarm application to guided munitions has a lot of advantages. For example, it becomes harder for a defense system to prevent munitions when the number of attackers increases. A larger area can be targeted with more agents. Moreover, unit cost can be decreased by using munitions without seeker, which we named naïve agent for this study. In conclusion, it is a cheap, destructive, and hard-to-prevent way to hit the desired area with a swarm of munition.

Informed agents are guides of a swarm since they have information about the target with the help of a seeker system on them. Naïve agents follow a trajectory that is shaped by informed agents. Naïve agents track a horizontal positions according to their neighbors. These positions are supplied by the potential function method according to the attraction and repulsion forces between the agents. At the vertical axis, naïve agents follow the position of the informed agent. Collision avoidance and uniformity are taken as a priority for naïve agents. In general, convoys of cars or military vehicles, a couple of housing placed nearby, or airplanes at a parking position are popular targets for a munition swarm. A cooperative guidance method with a formation controller can be applied to these types of target sets.

All the munitions are modeled and simulated with 6 degrees of freedom equation of motion. Navigation, guidance, and autopilot systems are modeled for each. Algorithms are analyzed and tested for various conditions, and the outputs of these simulations are plotted and investigated in Chapter 6. The total number of agents in the swarm and the number of informed agents in the swarm are studied by changing only one of them at a time. Effects of these two on the irregularity of horizontal positions, heading errors, and wideness metrics of the swarm are compared. It is seen that the addition of more agents makes it harder to organize the swarm at the point of regularity and heading angles, and the swarm follows a wider path naturally. Changing a naïve agent to an informed agent also creates irregularity but enhances the heading angle errors, and the swarm tends to stay away from each other a little.

The present study can be improved with the following works:

- Effects of sensor measurement errors in accelerometer and gyroscope can be added into the study, and the results might be investigated.
- Effect of the potential function parameters on the swarm trajectory and swarm parameters such as irregularity and wideness might be analyzed with several runs.
- Distribution around the informed agent trajectory might be shaped on the pitch axis according to determined shapes, not only in the horizontal plane.
- Data link is assumed as transferring the data without any delay for this study, delay of the data link might be modeled and analyzed.
- An algorithm to decrease the arrival time difference of the agents might be studied.

In this thesis study, a cooperative guidance method with formation control proposes uniform, safe, and collaborative flight while guiding the swarm toward the target. Moreover, horizontal uniformity provides uniform area destruction perpendicular to the closing direction, which is preferable for a target set positioned in line. Cooperation, orderliness, and safety of the swarm are observed with the 6 degrees of freedom model of each munition, which is created on MATLAB/SIMULINK application, and results of single and several runs are investigated in detail. According to these outputs, in all the cases, a successful flight trajectory for a swarm is noted.

REFERENCES

[1] K. Jens, D. R. Graeme and K. Stefan, “Swarm Intelligence in Animals and Humans”, Trends in Ecology and Evolution, vol. 25, no.1, pp.28- 34, 2010

[2] Çelikkanat, H., & Şahin, E. (2010). Steering self-organized robot flocks through externally guided individuals. *Neural Computing And Applications*, *19*(6), 849-865.

[3] Olfati-Saber, R., & Murray, R. (2002). DISTRIBUTED COOPERATIVE CONTROL OF MULTIPLE VEHICLE FORMATIONS USING STRUCTURAL POTENTIAL FUNCTIONS. *IFAC Proceedings Volumes*, *35*(1), 495-500.

[4] Ferrante, E., Turgut, A. E., Dorigo, M., & Huepe, C. (2013). Elasticity-based mechanism for the collective motion of self-propelled particles with springlike interactions: A model system for natural and artificial swarms. Physical Review Letters, 111(26).

[5] Antonelli, G., Arrichiello, F., & Chiaverini, S. (2008). Flocking for multi-robot systems via the null-space-based behavioral control. 2008 IEEE/RSJ International Conference on Intelligent Robots and Systems.

[6] He, L., Bai, P., Liang, X., Zhang, J., & Wang, W. (2018). Feedback formation control of UAV swarm with multiple implicit leaders. Aerospace Science and Technology, 72, 327–334.

[7] Mahmood, A., & Kim, Y. (2015). Leader-following formation control of quadcopters with heading synchronization. Aerospace Science and Technology, 47, 68–74.

[8] Nouyan, S., Campo, A., & Dorigo, M. (2007). Path formation in a robot swarm. Swarm Intelligence, 2(1), 1–23. https://doi.org/10.1007/s11721-007-0009-6

[9] C. Ma and Q. Zeng, "Distributed formation control of 6-DOF autonomous underwater vehicles networked by sampled-data information under directed topology," Neurocomputing, vol. 154, pp. 33-40, 2015.

[10] Song, Z., & Mohseni, K. (2013). Cooperative Underwater Localization in Ocean Currents. AIAA Guidance, Navigation, and Control (GNC) Conference.

[11] Erer, K. S., & Tekin, R. (2016). Impact Time and Angle Control Based on Constrained Optimal Solutions. Journal of Guidance, Control, and Dynamics, 39(10), 2448–2454.

[12] Erer, K. S., & Merttopçuoglu, O. (2012). Indirect Impact-Angle-Control Against Stationary Targets Using Biased Pure Proportional Navigation. Journal of Guidance, Control, and Dynamics, 35(2), 700– 704.

[13] Erer, K. S., & Ozgoren, M. K. (2013). Control of impact angle using biased proportional navigation. AIAA Guidance, Navigation, and Control (GNC) Conference.

[14] Byung Soo Kim, Jang Gyu Lee, & Hyung Seok Han. (1998). Biased PNG law for impact with angular constraint. IEEE Transactions on Aerospace and Electronic Systems, 34(1), 277–288.

[15] In-Soo Jeon, Jin-Ik Lee, & Min-Jea Tahk. (2006). Impact-time-control guidance law for anti-ship missiles. IEEE Transactions on Control Systems Technology, 14(2), 260–266.

[16] Shiyu, Z., & Rui, Z. (2008). Cooperative Guidance for Multimissile Salvo Attack. Chinese Journal of Aeronautics, 21(6), 533–539.

[17] Saleem, A., & Ratnoo, A. (2016). Lyapunov-Based Guidance Law for Impact Time Control and Simultaneous Arrival. Journal of Guidance, Control, and Dynamics, 39(1), 164–173.

[18] Özgören, M. K., Kinematics of General Spatial Mechanical Systems, Wiley, Hoboken, NJ, 2020, Chaps. 1–4.

[19] B. Etkin, Dynamics of atmospheric flight. Dover Publications, 2005.

[20] Ogata, K., & Ogata, K. (2002). Solutions manual, Modern Control Engineering, Fourth Edition. Prentice Hall.

[21] Anderson, J. D. (2001). Fundamentals of aerodynamics. Mc-Graw Hill.

[22] L. Keller and E. Gordon, The Lives of Ants, Oxford University Press, Oxford 2009.

[23] Ahmed, H., & Glasgow, J. (2012). Swarm intelligence: concepts, models and applications. School Of Computing, Queens University Technical Report.

[24] Gazi, V., Koksal, M. I., & Fidan, B. (2007). Aggregation in a swarm of non-holonomic agents using artificial potentials and sliding mode control. 2007 European Control Conference (ECC).

[25] Campion, M., Ranganathan, P., & Faruque, S. (2018, May). A review and future directions of UAV swarm communication architectures. In 2018 IEEE international conference on electro/information technology (EIT) (pp. 0903-0908). IEEE.

[26] Bibuli, M., Bruzzone, G., Caccia, M., Gasparri, A., Priolo, A., & Zereik, E. (2014). Swarm-based path-following for cooperative unmanned surface vehicles. Proceedings of the Institution of Mechanical Engineers, Part M: Journal of Engineering for the Maritime Environment, 228(2), 192-207.

[27] Marin, N., & Spataru, P. (2010). The role and importance of UAV within the current theaters of operations. INCAS Bull, 2, 66-74.

[28] Muchiri, G. N., & Kimathi, S. (2022, April). A review of applications and potential applications of UAV. In Proceedings of the Sustainable Research and Innovation Conference (pp. 280-283).

[29] V. Gazi and K. M. Passino, Swarm Stability and Optimization, Springer Verlag, January 2011.

[30] V. Gazi and K. M. Passino, “A Class of Attraction/Repulsion Functions for Stable Swarm Aggregations," International Journal of Control, Vol. 77, No. 18, pp. 1567-1579, December 2004.

[31] Barnes, L., Fields, M., & Valavanis, K. (2007, June). Unmanned ground vehicle swarm formation control using potential fields. In 2007 Mediterranean Conference on Control & Automation (pp. 1-8). IEEE.

[32] Shneydor, N. A. (1998). Missile guidance and pursuit: kinematics, dynamics and control. Elsevier.

[33] Yamasaki, T., & Balakrishnan, S. (2010, August). Triangle intercept guidance for aerial defense. In AIAA Guidance, Navigation, and Control Conference (p. 7876).

APPENDICES

A. Effect of Informed Agent Number Outputs

At the part 6.3.2 Effect of Informed Agent Number, results for different runs are plotted. Horizontal trajectory outputs for 3,13 and 23 informed agents cases are plotted as shown in Figure 59. Informed agents are shown with dashed lines.

Figure 59 Horizontal trajectories for 23 agents with 3 informed agents

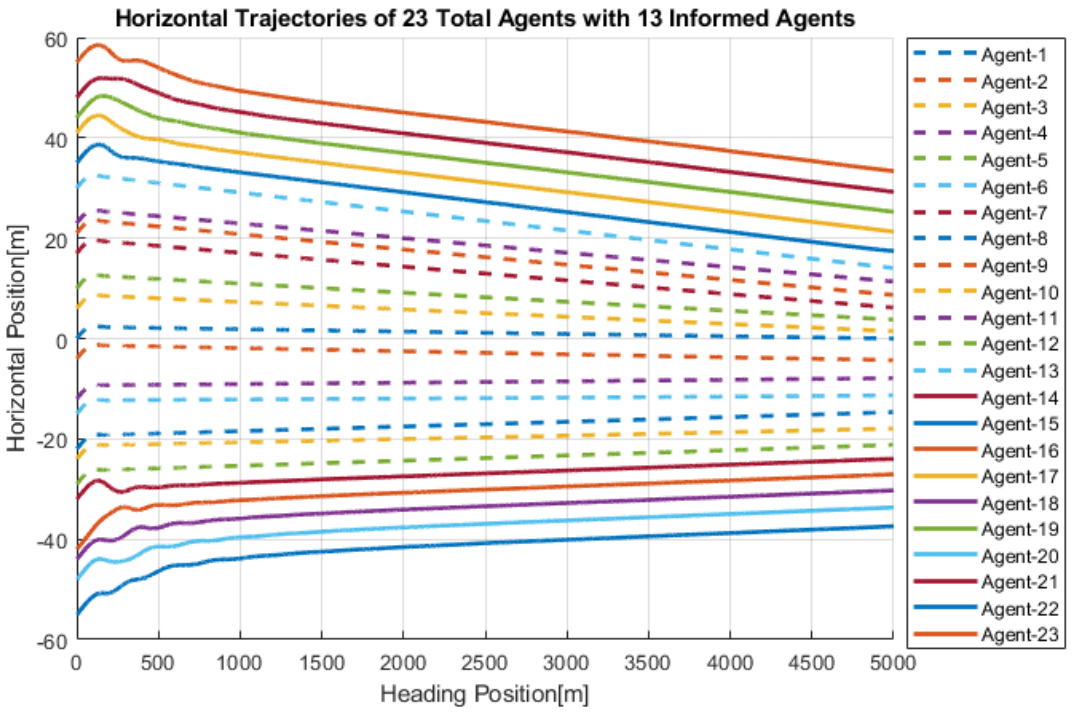

Figure 60 Horizontal trajectories for 23 agents with 13 informed agents

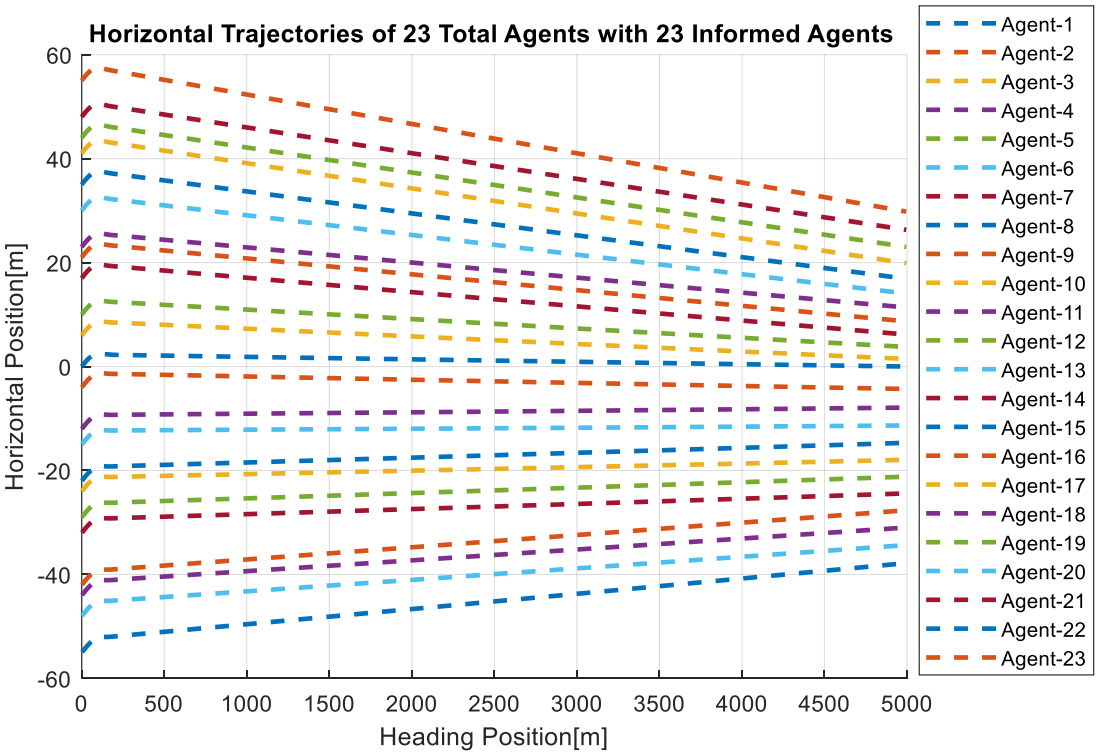

Figure 61 Horizontal trajectories for 23 agents with 23 informed agents

B. Effect of Total Agent Number Outputs

At the part 6.3.1 Effect of Total Agent Number, results for different runs are plotted. Horizontal trajectory outputs for 5, 11, 17, and 23 total agent cases are plotted as shown in Figure 62.

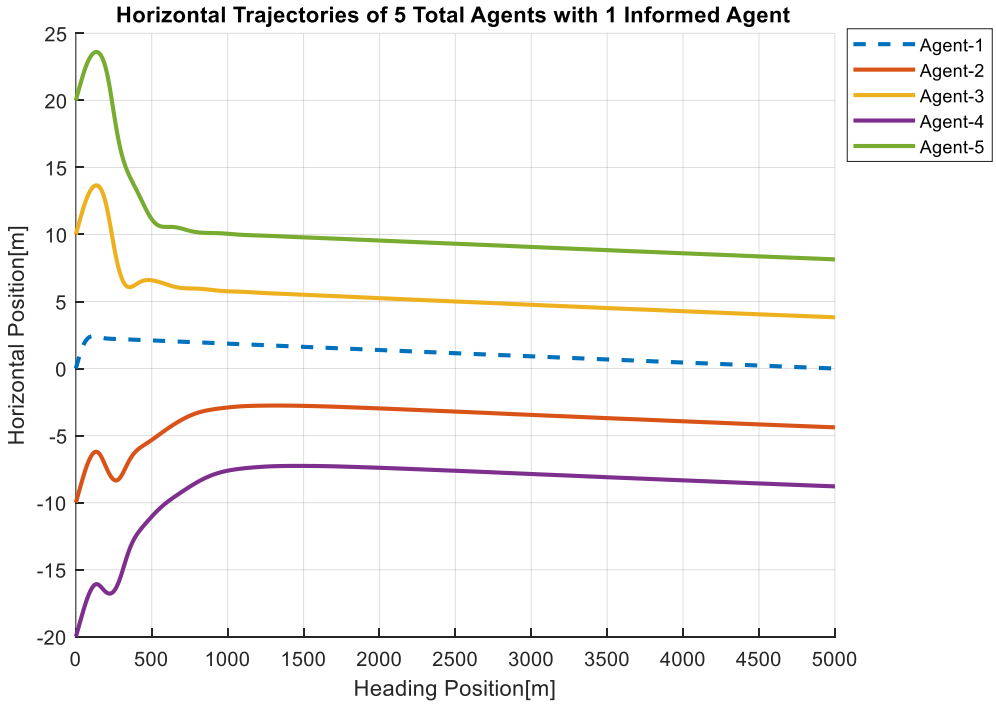

Figure 62 Horizontal trajectories for 5 agents with 1 informed agent

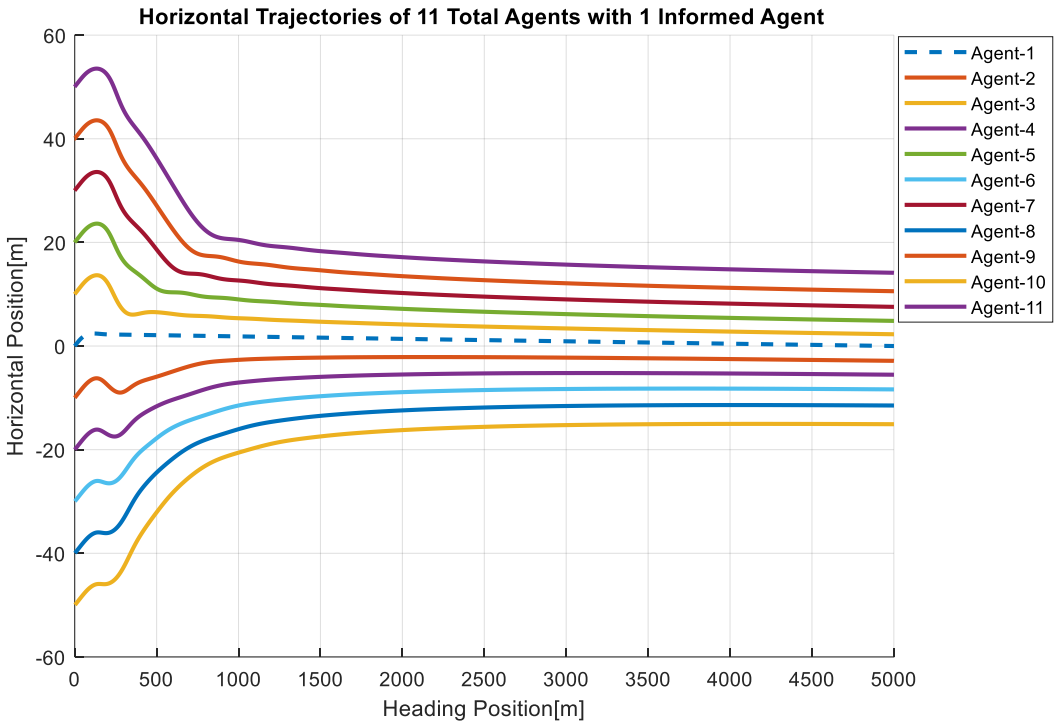

Figure 63 Horizontal trajectories for 11 agents with 1 informed agent

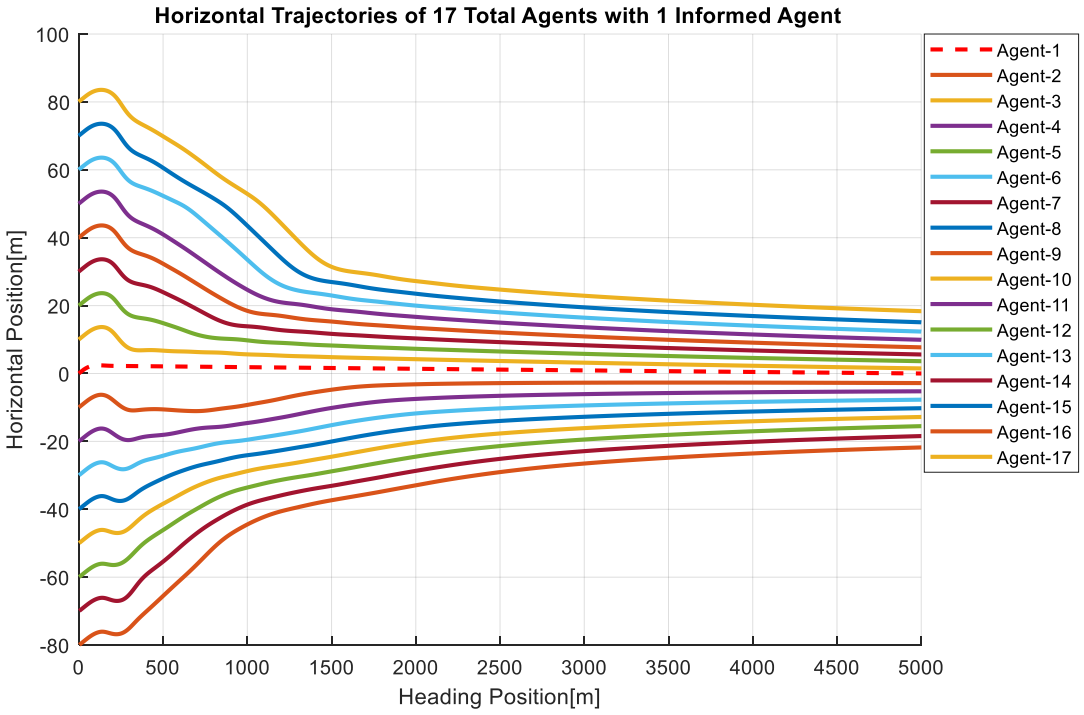

Figure 64 Horizontal trajectories for 17 agents with 1 informed agent

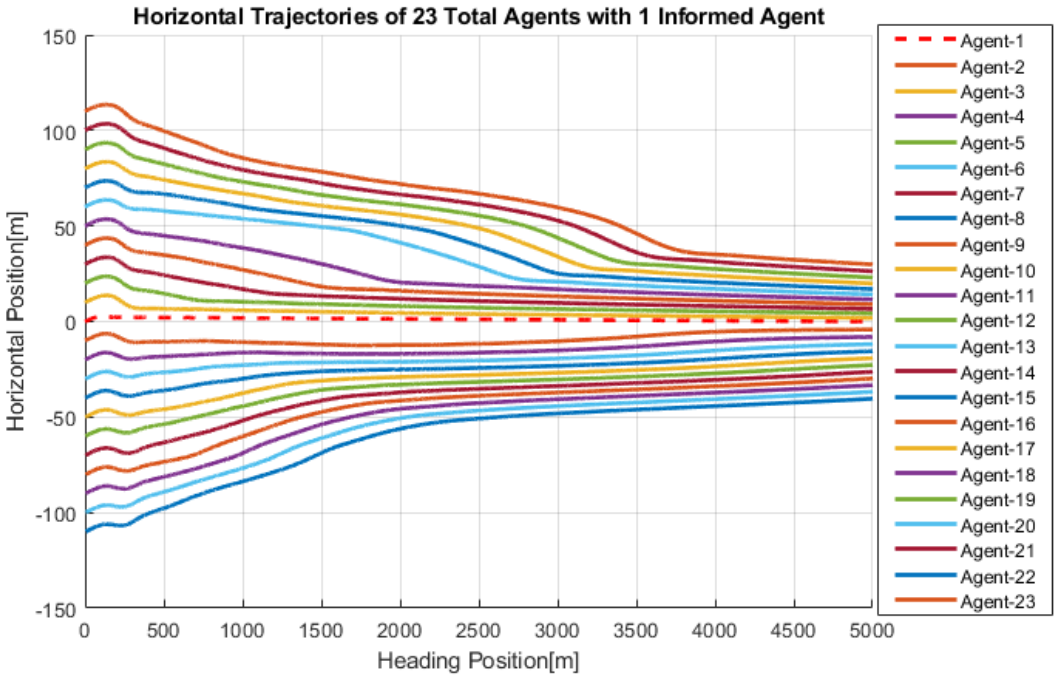

Figure 65 Horizontal trajectories for 23 agents with 1 informed agent